

The University of Nottingham



CBS
CENTRE FOR BIOMOLECULAR SCIENCES

Supported by wellcome trust

Wellcome Trust: Antimicrobials and Antimicrobial Resistance

Tom Armstrong MChem (Hons)

Thesis submitted to the University of Nottingham for the degree of

Master of Research

September 2017

Abstract

The issue of antimicrobial resistance is one that threatens the very existence of humanity. For this reason it should be subject to increasingly intense investigation by the scientific community. The aims of this work was to explore two projects focused on creating novel treatments and therapies to be used as antimicrobial strategies.

The first project was focused on the synthesis of novel anti-tuberculosis (TB) drugs, in order to address the increasing issue of multi and extensively drug-resistant TB. To this end, a partial synthesis of two iminosugar molecules was carried out, using a ring closing metathesis as a key step to form the desired 5-membered ring. A similar approach was taken to try and synthesise a furanose equivalent but this reaction was unsuccessful. These iminosugars have been shown to act as moderate inhibitors of the Galactofuranosyl Transferase 2 (Gal*f*T2) pathway in *Mycobacterium tuberculosis*. Derivative structures of these iminosugars were proposed for future synthesis in order to explore the potential of iminosugars as GalfT2 inhibitor class.

A concise synthesis of the biologically active cerebrosides compound **KRN7000** is reported. This synthesis uses a TBAI mediated glycosylation step to deliver, exclusively, the desired α-galactoside. The synthesis of an azide-containing analogue was investigated but installation of the azide functionality via a Mitsunobu reaction proved unsuccessful. Two PTAD linkers were designed which could be attached to 6-deoxy-6-azido-α-GalCer in order to investigate further conjugation to the flagellin through the PTAD moiety. A partial synthesis of these PEG compounds is reported.

Acknowledgements

I would like to begin by thanking the Wellcome Trust for funding this research and its continued commitment to improving the lives of people around the world.

Thank you to Professor Thomas and Dr Cox for providing interesting and stimulating projects, as well as providing useful feedback. Additional thanks to Dr Stocks for his helpful comments and feedback on this thesis. I also wish to extend my gratitude to the analytical services staff at the University of Nottingham and Birmingham, without whom the analytical facilities would not function. Thank you also to the Thomas and Cox research groups for making me feel welcome during my time spent working with them.

Contents

	Page
Abstract	i
Acknowledgements	ii
Contents	iii
Abbreviations	iv
Chapter 1	
The Current State of Antimicrobial Resistance	1
Chapter 2	
Restarting the Pipeline: The need for new anti-TB drugs	8
Targeting TB: Development of new inhibitors of *Mycobacterium tuberculosis* galactofuranosyl transferase Gal*f*T2	14
Chapter 3	
CD1d-restricted NKT Cells: The immune system's Swiss	27
Army Knife	
Synthesis of **KRN7000** and design and partial synthesis of novel azido-α-GalCer compounds containing PTAD linker motifs.	30
Chapter 4	
Future Perspectives and Concluding Remarks	47
Appendix	
References	51
Experimental Procedures	55

Abbreviations

α-GalCer	α-galactosyl ceramide
AMR	Antimicrobial resistance
CSA	Camphorsulfonic Acid
DCC	*N,N'*-Dicyclohexylcarbodiimide
DIAD	Diisopropyl azodicarboxylate
DMAP	4-Dimethylaminopyridine
DMP	Dess-Martin periodinane
DMSO	Dimethyl sulfoxide
DPPA	Diphenylphosphoryl azide
DS-TB	Drug-susceptible tuberculosis
EDCI	1-Ethyl-3-(3-dimethylaminopropyl)carbodiimide
ELIPSOT	Enzyme-linked ImmunoSpot
EMB	Ethambutol
ESI	Electrospray ionisation
Et_3N	Triethylamine
Gal*f*	Galactofuranose
Gal*p*	Galactopyranose
HMDS	Hexamethyldisilazane
HIV	Human immunodeficiency virus
HR-MS	High resolution mass spectrometry
Im	Imidazole
INH	Isoniazid
MDR-TB	Mutli-drug resistant tuberculosis
MHC	Major histocompatibility complex
MS	Molecular sieve
MsCl	Methanesulfonyl chloride
NADH	Nicotinamide adenine dinucleotide
NAG-NAM	N-acetyl glucosamine– N-acetyl muramic acid
NK	Natural killer cells
NKT	Natural killer T cells
NMR	Nuclear magnetic resonance
PCC	Pyridinium chlorochromate
PEG	Polyethylene glycol
PTAD	4-phenyl-1,2,4-triazole-3,5-dione
PZA	Pyrazinamide

RCM	Ring closing metathesis
RMP	Rifampicin
RT	Room temperature
SAR	Structure activity relationship
SPR	Surface plasmon resonance
TB	Tuberculosis
TBAF	Tetra-*n*-butylammonium fluoride
TBAI	Tetra-*n*-butylammonium iodide
TBDPSCl	*Tert*-butyl diphenyl silyl chloride
^{t}Bu	*Tert*-butyl
TCR$\beta\delta^{-/-}$	T cell receptor deficient
TDR-TB	Totally drug-resistant tuberculosis
THF	Tetrahydrofuran
TFA	Trifluoroacetic acid
TMSCl	Trimethyl silyl chloride
TMSI	Trimethyl silyl iodide
TsCl	Tosyl chloride
UDP-Gal*f*	Uridine diphosphate galactofuranose
UDP-Gal*p*	Uridine diphosphate galactopyranose
USD	United States Dollar
WHO	World Health Organisation
XDR-TB	Extensively drug-resistant tuberculosis

Chapter 1
The Current State of Antimicrobial Resistance

The discovery and application of antibiotics represents one of the most transformative discoveries in the history of science.[1-3] The dawning of the antibiotic age has helped to save the lives of countless people. Not only have antibiotics allowed people to overcome infectious diseases, they have also facilitated the expansion of more invasive surgeries and organ transplants.[4] Such surgeries had previously been limited by significant concerns regarding the absence of an effective means to fight infections which can arise during such major surgery. It is no over exaggeration to say that antibiotics revolutionised medicine.

Regrettably, the use of antibiotics is inextricably linked with the emergence of resistance which lessens, and in many cases, abolishes their efficacy.[5-7] The evidence of the severity of antimicrobial resistance (AMR) is incontrovertible. In recent years, a database has been established which is dedicated to tracking the prevalence of genes associated with AMR, with the current total standing in excess of 20,000 potential resistance genes, operating through over 400 mechanisms.[8] Until now the potential doomsday scenario of blanket antibiotic resistance has been avoided due to the fact that these resistance determinants are found in much lower numbers in pathogens. However, if humanity does not act to adjust its current course we will creep increasingly closer to a return to *the dark ages,* and a post-antibiotic era, where infections will once again represent a death sentence.

Such is the danger posed by AMR, the former British Prime Minister, David Cameron, commissioned an all-encompassing report into the potential implications of widespread AMR. This review was headed-up by the economist Jim O'Neill, who upon invitation to chair the review remarked "Why should an

economist lead this? Why not a health economist?" the answer to this question soon became apparent as the review investigated the potential macro-economic impacts that would be associated with the emergence of AMR.[9] When O'Neill looked at the financial cost of AMR, his projections showed worrying forecasts for the health of the economy. Working with KPMG and Rand, O'Neill forecasted that, by 2050, the loss of global productivity would total 100 trillion US Dollars (USD). Such damage to economies would have a cyclical impact on the progression of AMR as it reduces governments abilities to act and invest in new treatments, meaning diseases become more troublesome. More significant than the financial implications is the human cost of AMR. O'Neill predicted that, without significant policy efforts to curtail the spread of AMR, global deaths would reach 10 million per annum by 2050. This is a staggering number and eclipses the combined number of annual deaths related to all forms of cancer. It is often the case that such projections are taken with a pinch of salt, due to the belief that there is a tendency is to overstate impacts, however O'Neill believes these forecasts are overly conservative, suggesting the actual impact could be far greater. Indeed, in the 19 months it took to carry out the review, several new forms of resistance emerged, highlighting the rate at which the situation is worsening.

The issue of AMR is far from a modern problem, sulphonamides, the first effective antimicrobial, introduced in 1937 were plagued by therapeutic resistance. Resistance to sulphonamides was first reported in the late 1930s and the same resistance mechanisms are still observed in clinical isolates 80 years later.[10-12]

For many people, Alexander Fleming's discovery (1928) and introduction of Penicillin (1940) heralded the dawn of the golden age for antibiotics, with the next 5-6 decades seeing rapid expansion and progress in the field of antibiotics. This led to the discovery and introduction of numerous different classes of antibiotics, these are summarised in Table 1.[13]

Table 1. Commonly used antibiotics, their biological targets and the basis for bacterial resistance to them. (Adapted from *Zaman et al.*[13])

Compound Class	Example(s)	Biological Target	Resistance Mechanism(s)
Aminoglycosides	Gentamicin, streptomycin	Translation	Phosphorylation, acetylation, nucleotidylation, efflux, target mutation
β-Lactams	Penicillins, cephalosporins, monobactams	Peptidoglycan biosynthesis	Hydrolysis, efflux, target mutation
Cationic Peptides	Colistin	Cell membrane	Efflux, target mutation
Glycopeptides	Vancomycin, teicoplanin	Peptidoglycan biosynthesis	Altered peptidoglycan biosynthesis pathway
Lincosamides	Clindamycin	Translation	Nucleotidylation, efflux, target mutation
Lipopeptides	Daptomycin	Cell membrane	Target mutation
Macrolides	Erythromycin, azithromicin	Translation	Hydrolysis, glycosylation, phosphorylation, efflux, target mutation
Oxazolidinones	Linezolid	Translation	Efflux, target mutation
Phenicols	Chloramphenicol	Translation	Acetylation, efflux, target mutation
Pyrimidines	Trimethoprim	C_1 metabolism	Efflux, target mutation
Quinolones	Ciprofloxacin	DNA Replication	Acetylation, efflux, target mutation
Rifamycins	Rifampin	Transcription	ADP-ribosylation, efflux, target mutation
Streptogramins	Synercid	Translation	C-O lyase, acetylation, efflux, target mutation
Sulfonamides	Sulfamethoxazole	C_1 metabolism	Efflux, target mutation
Tetracyclines	Minocycline, tigecycline	Translation	Monooxygenation, efflux, target mutation

While Fleming's description of the clinical efficacy of penicillin in 1940 was widely reported and is well known, he also reported a second discovery in the same year, which saw significantly less coverage.[14] Fleming and his team identified a bacterial penicillinase enzyme which conferred resistance to penicillin, this was several years before penicillin saw widespread use outside of a testing environment.[15]

Indeed, in the closing remarks of his 1945 Nobel Prize Lecture, Fleming warned, that without proper care, there was significant potential for bacteria to accumulate resistance to penicillin. This warning appears all the more prescient given the forecasts made in the O'Neill report.[16]

In the years since penicillin's introduction, there has been a dramatic shift in the landscape of antibiotics and AMR, with rapid expansions being seen in both areas (Fig. 1).[17,18]

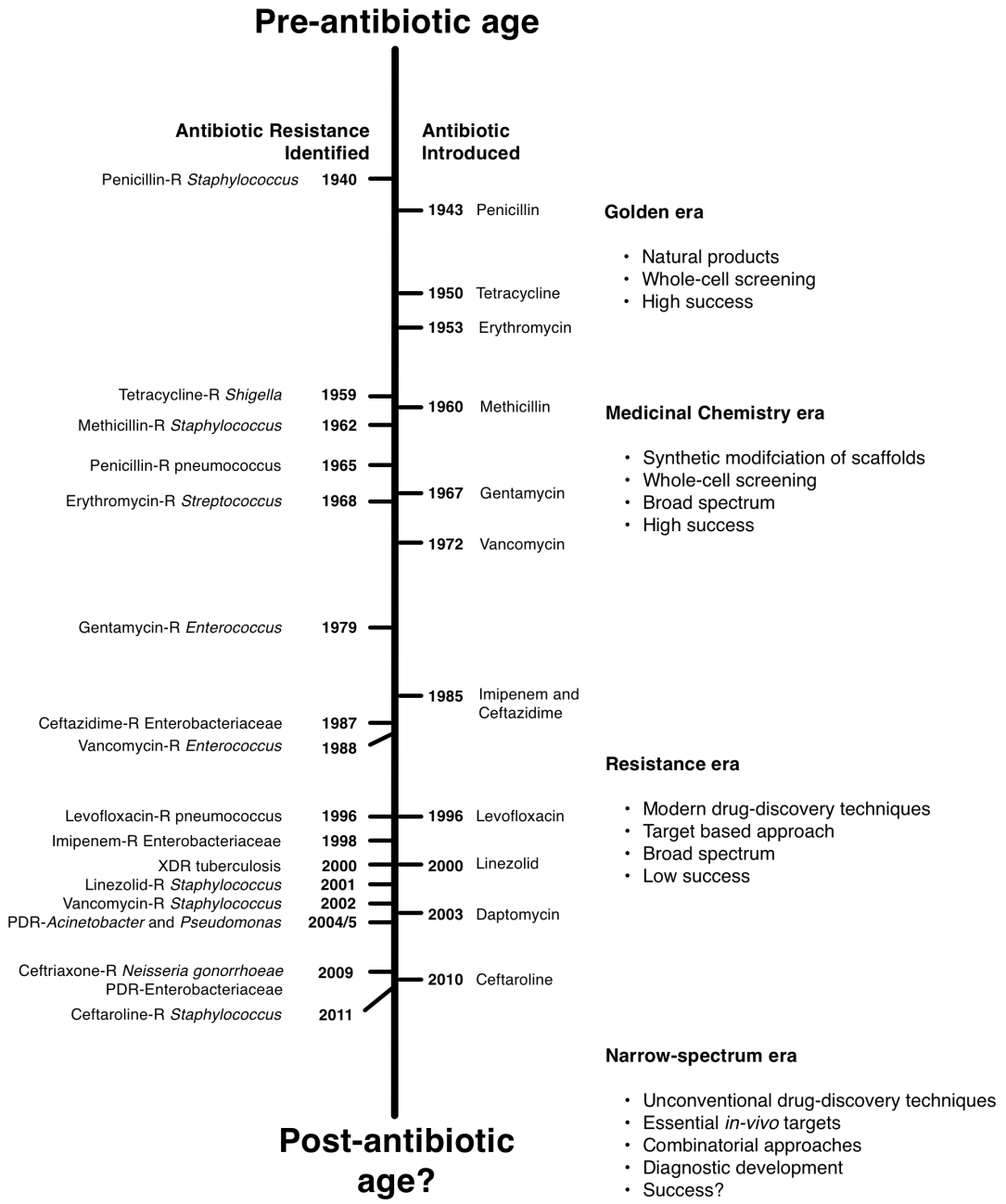


Fig. 1. Timeline showing the introduction of various milestone antibiotics and also the first instances of significant resistances being detected. Also shown is a summary of the various antibiotic drug discovery approaches which have been adopted over the course of the last 70 years. (Adapted from Lewis.[18])

This timeline shows that, especially in the last 20 years, the rate at which AMR bacteria are developing has accelerated dramatically. In some instance, for example in the case of Linezoid, the introduction of an antibiotic can be almost immediately concomitant with the emergence of resistant bacteria.

In his review, O'Neill identified numerous factors which need to be addressed in order to slow the march of AMR. O'Neill first highlighted the need to reeducate the general public, many of whom often, unnecessarily, demand antibiotics from their doctors and GPs. The level of public reeducation needed was seen as analogous to the campaigns required to reduce smoking rates, or to get people to wear seatbelt in cars. At the time these seemed like monumental tasks, but evidence shows significant adoption of the more positive behaviour, suggesting that such a reeducation programme would not be in vain.

Another factor identified by O'Neill was the need for improved sanitation, this is an issue which is particularly prominent third world countries. The fact that most antibiotics are excreted unmetabolised means that if sanitation systems are not sufficient, the sewers become a breeding ground for AMR bacteria.

One of the most concerning issue raised in the review was the gross misuse of antibiotics in agriculture, the level of antibiotics used in livestock is staggering. Clearly, there are instances where antibiotic use is required as a means to fight infections in livestock in order to ensure animal health & safety and thus maintain global food security. However, O'Neill's report highlighted the widespread abuse of antibiotics in agriculture. One of O'Neill's most startling findings was that, in the US, of the antibiotics designated as 'medically important for humans' by the FDA, in excess of 70% of their usage (by weight) comes from agriculture. It is likely that this trend could be mirrored around the world, but sufficient data is not readily available, or worse, is simply not recorded. The intensive nature of modern farming techniques means that oftentimes there are large numbers of animals living in close proximity and in unhygienic conditions. These conditions act as a reservoir for resistance and significantly accelerate its spread. O'Neill made three recommendations which he said were needed in order to prevent agriculture contributing to the escalation of AMR:

1. Introduction of 10-year targets to reduce unnecessary antibiotics use in agriculture.
2. Restrictions and/or bans on the use of highly critical antibiotics in livestock
3. Seek to improve the transparency in the supply chain with regards to suppliers' use of antibiotics in livestock.

Clearly the implementation of new policies is a key factor in the fight against AMR. However, of equal importance is the need for innovation within the scientific community to drive the creation of new drugs and treatments in order to meet the growing demands. The aim of this work is to explore two projects, both unique in scope, but ultimately contributing to the efforts to develop new antibiotic strategies.

Chapter 2

Restarting the Pipeline: The need for new anti-TB drugs

Mycobacterium tuberculosis was first identified as the causative agent of tuberculosis (TB) by Robert Koch in 1882 and since then the global TB epidemic has progressed in a relentless fashion.[19] In 2015 there were 10.4 million new cases of TB reported globally, more than ever before.[20,21] This high infection rate reflects the relative ease with which TB can spread. Transmission can be achieved by the inhalation of only a few droplets, no more than 5 μm in diameter, containing as few as 1-3 bacilli.[22] In addition to the increasing infection rate, it is estimated that roughly one-third of the global population is infected with dormant or latent TB, which carries with it the lifelong risk of reactivation. This reactivation risk is significantly increased in individuals with a compromised immune system, making TB a leading killer in those with human immunodeficiency virus (HIV).[23,24] The incompatibility of rifampicin and antiretroviral drugs presents a particular problem for HIV sufferers, this will be discussed in more detail later.

Treatment of individuals with drug-susceptible TB (DS-TB) relies on a two-phase combination therapy. The first phase of treatment involves rifampicin (RMP, **1**), isoniazid (INH, **2**), pyrazinamide (PZA, **3**) and ethambutol (EMB, **4**) over a two month period, this is then followed by a continuation-phase of RMP and INH for a further four months (Fig 2).[25,26]

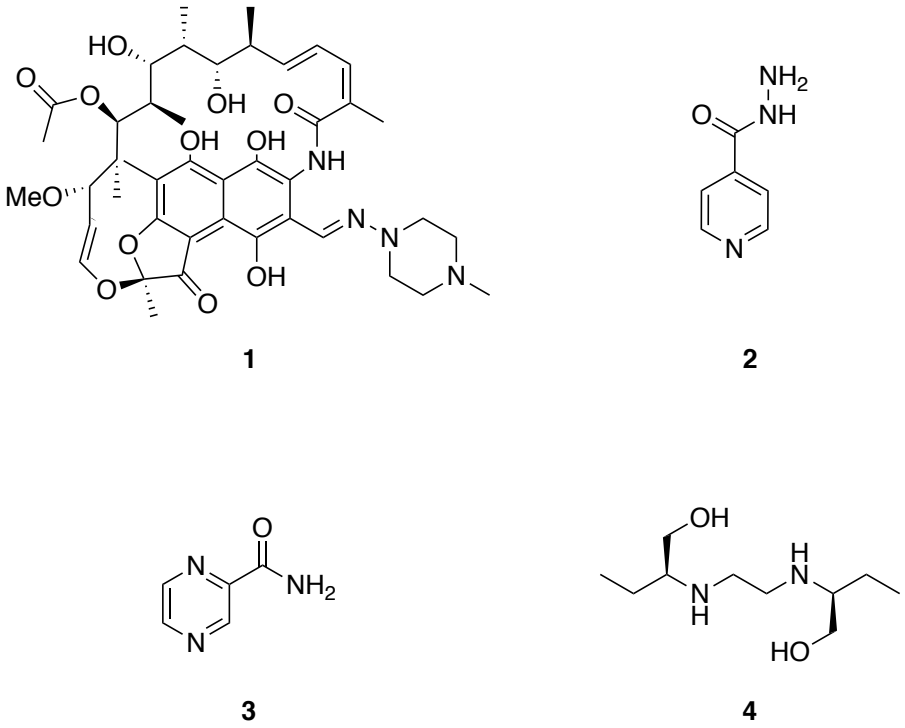


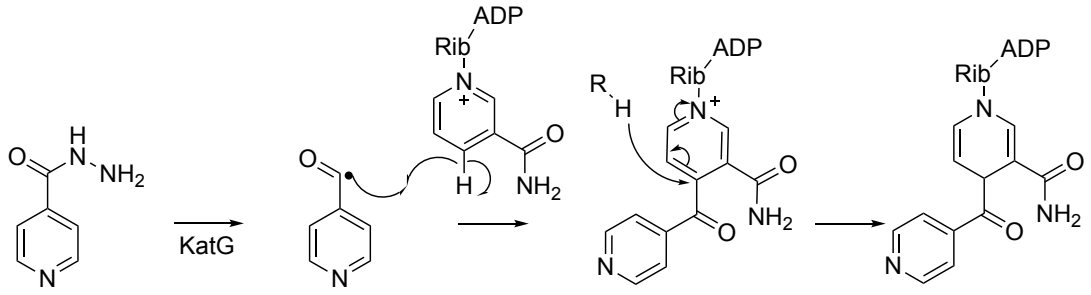
Fig. 2. The structures of the four drugs which make up the anti-TB regimen. Rifampicin (1), Isoniazid (2), Pyrazinamide (3) and Ethamobutol (4)

In most cases (95%) people with DS-TB can be cured in six months by this four drug regimen.[27] However this treatment course is complicated by the fact that TB tends to be particularly prevalent in developing countries where access to good healthcare facilities and adequate drug supply is limited.[28] Another issue associated with the treatment of DS-TB is its protracted nature, which brings with it problems of patient compliance, diminishing the effectiveness of the treatment regimen.[29-31]

As with other infectious bacterial disease, the issue of AMR in TB is one that is on the rise. The World Health Organisation (WHO) recently reported that 9.5% of TB infections present resistance to at least two of the front-line drugs: INH and RMP.[32,33] Infections resistant to these two particular drugs are known as multi-drug resistant (MDR-TB). MDR-TB infections require a much more gruelling treatment course lasting, up to 2 years, with a combination of as many as 10 drugs.[34] Of these 10 drugs, only 4 were originally intended to treat TB leading to suboptimal

therapy conditions. The suboptimal conditions result in around 30% of MDR-TB patient treatments ending in failure.[27,35] As previously mentioned, incomplete treatment is a significant issue with TB and has also been shown to be a significant driver of MDR-TB infections. Of the DS-TB patients who relapse, 20.5% of them present a newly MDR-TB infection.

One of the drugs which forms the cornerstone of the anti-TB drug regiment is INH (**2**). INH is a pro-drug activated by the enzyme KatG, this activated compound is then able to inhibit InhA in *Mycobacterium*. KatG is a multi-function peroxidase which also displays other enzymatic activities including β-nicotinamide adenine dinucleotide (NADH) oxidase and peroxynitritase. A detailed discussion of the elucidation of KatG's mechanism for INH activation and it's subsequent activity is provided by Timmins *et al.* and the accepted pathway is shown in Scheme 1.[36]



Scheme 1. The pathway through which INH is able to inhibit InhA. First INHA is converted an isonicotinic acyl radical (5) by KatG. This radical then forms an INH-NAD(P)$^+$ adduct (6) *via* a Minisci addition reaction, this radical cation is then terminated by the addition of an electron giving INH-NAD(P) (7)

InhA has been shown to catalyse the NADH-specific reduction of the 2-trans-enoyl-acyl carrier protein (enoyl-AcpM), this is a crucial step in fatty acid elongation, which plays a key role in the biosynthesis of TB's cell wall. The INH-NADH(P) adduct, **7**, binds tightly to InhA thereby blocking recognition of its natural

substrate, enoyl-AcpM, and inhibiting InhA's biological function of mycolic acid synthesis. These acids form a key part of the complex TB cell wall and INH's potent activity explains why it is one of the key drugs in the anti-TB treatment regimen. Resistance to INH has been found to be primarily mediated by mutations in KatG, rather than InhA.[37,38] Mutation in KatG prevents the conversion of the INH pro-drug into its active form, thus diminishing its activity. These mutations do not impact on KatG's ability to fulfil its biological role, so carry a low fitness cost to the organism.

RMP (**1**) is a complex, cyclic natural product antibiotic which was first introduced in 1972. Due to RMP's efficient antimicrobial action, alongside INH, it is used throughout the regimen.

RMP mediates its anti-TB activity through binding to the β-subunit of RNA polymerase, which inhibits the elongation of messenger RNA.[39] One of the major issues associated with treating TB is the difficulty in successfully treating both active and dormant bacilli at the same time. It is RMP's ability to effectively combat latent and active TB which makes it such a powerful anti-TB drug.[40]

The principal driver of RMP resistance in TB is mutation in the rpoB gene. This gene is responsible for encoding the β-subunit of RNA polymerase.[41] Mutations in the gene results in conformational changes in the polymerase which significantly lower the binding affinity of RMP, conferring resistance upon the organism.[42]

The emergence of TB strains with dual resistance to INH and RMP presents a significant challenge to healthcare systems and is an issue which must be addressed as a matter of priority. The severe need for new antibiotics to defeat MDR-TB has been exacerbated by the emergence of extensively drug-resistant TB (XDR-TB).[43] These are MDR-TB strains which also present resistance to

fluoroquinolones and injectable, second-line antibiotics such as aminoglycosides. [44] Individuals suffering with XDR-TB face a bleak outlook, with very few options available to treat their infections. In addition to MDR and XDR-TB, there have also been cases of totally drug-resistant TB (TDR-TB) reported in parts of Asia, Africa and Eastern Europe.[45]

As has previously been mentioned, TB infections prove particularly problematic for those also infected with HIV, so much so that one in four deaths among HIV-positive individuals are attributed to TB infections.[46] The co-infection of HIV-positive people with TB causes significant complications to the treatment regimen for a number of reasons 1) the increased pill burden reduces patient compliance; 2) drug-drug interactions result to a reduction in the concentration of antiretroviral drugs, to a sub-therapeutic level; 3) Cumulative toxic side effects from overlapping drug courses.

The reason for the significant reduction in the plasma concentration of antiretrovirals, when administered alongside rifampicin, is due to the rifampicin-induced up-regulation in expression of the hepatic cytochrome (CYP) P450 oxidase system.[47] The increased level of CYP450 results in the metabolism of many HIV protease inhibitors, so much so that even in the presence of CYP450 inhibitors the drug concentrations fall to a sub-therapeutic level.[48]

Through the combination of increasingly aggressive strains of TB and a dearth of new compounds in the anti-TB pipeline, the point has been reached where the prospect of a *post-antibiotics era*, for TB infections, is a very real possibility. This means there is a clear need for new molecules harbouring distinct anti-TB properties (Fig 2).

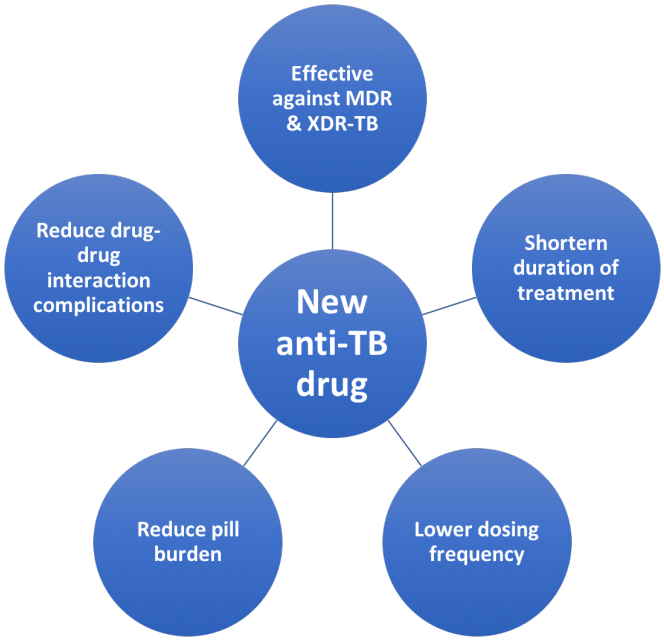
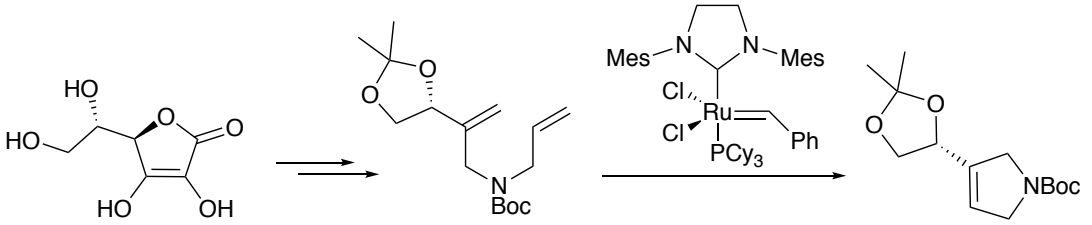


Fig. 2. The desired profile of a new anti-TB drug.

The first project will investigate the potential use of iminosugars as novel inhibitors of Galactofuranosyl transferase (Gal*f*T) in *Mycobacterium tuberculosis*. Gal*f*T is a key enzyme in the biosynthetic pathway of the TB cell wall. This means that, despite being relatively unexplored, it represents an attractive target for the development of novel anti-TB drugs. This project will focus on the synthesis of an iminosugar which acts as a synthetic mimetic of the enzyme's natural substrate. The structure can then be investigated and subject to structure activity relationship (SAR) modifications. This project represents a more traditional medicinal chemistry approach to the problem of AMR. That is to say it focuses on the identification of a target and the rational design of molecules which can address it.

Targeting TB: Development of new inhibitors of *Mycobacterium tuberculosis* galactofuranosyl transferase Gal*f*T2



A partial synthesis of two iminosugar molecules has been carried out using a ring closing metathesis as a key step to form the desired 5-membered ring. A similar approach was taken to try and synthesise a furanose equivalent but this reaction was unsuccessful. These iminosugars have been reported to be moderate inhibitors of the Galactofuranosyl Transferase 2 (GalfT2) pathway in Mycobacterium tuberculosis. Derivative structures of these iminosugars were proposed for future synthesis in order to explore the potential of iminosugars as GalfT2 inhibitor class.

Introduction

It is an inescapable fact that the rising spectre of AMR represents one of the greatest existential threats to humanity.[5,49,50] Alongside climate change and meeting the demands of a growing population, AMR will begin to place increasing strain on the systems designed to protect against it. The potential scale of the problem was recently summarised in the O'Neil report, which was commissioned by the British government. O'Neil's report painted a stark picture if new means to combat bacterial infections are not uncovered The report highlighted the twin impacts of AMR, firstly the human cost which was estimated to reach 10 million lives lost per year, by 2050, as a result of resistant infections. In addition to this, O'Neil estimated the cumulative impact to the global economy would approach a staggering $100 trillion over the next 40 years.

Mycobacterium tuberculosis infections are responsible for the pathogenesis of various diseases, including leprosy and TB.[51-54] The World Health Organisation (WHO) recently reported that TB ranked as one of the top 10 global killers, TB is

also the most common cause of death for AIDS sufferers. The issue of TB is particularly troublesome in less economically developed nations, of the 1.8 million annual deaths, 60% of them are accounted for by: India, Indonesia, China, Nigeria, Pakistan and South Africa. With incidence of drug-resistant TB on the rise, it is imperative that new anti-TB drugs are developed in order to avoid further escalation of the global TB problem.

One of the most attractive targets for anti-TB drugs is the cell wall biosynthesis pathway, as it represents an essential process for cell survival and proliferation.[17,55] TB, like all *Mycobacteria*, have a unique glycolipid cell wall which provides the cell with substantial protection from the environment. The structure of the TB cell wall consists of three distinct units, composed of peptidoglycan, arabinogalactan and mycolic acids (Fig 3).[56, 57]

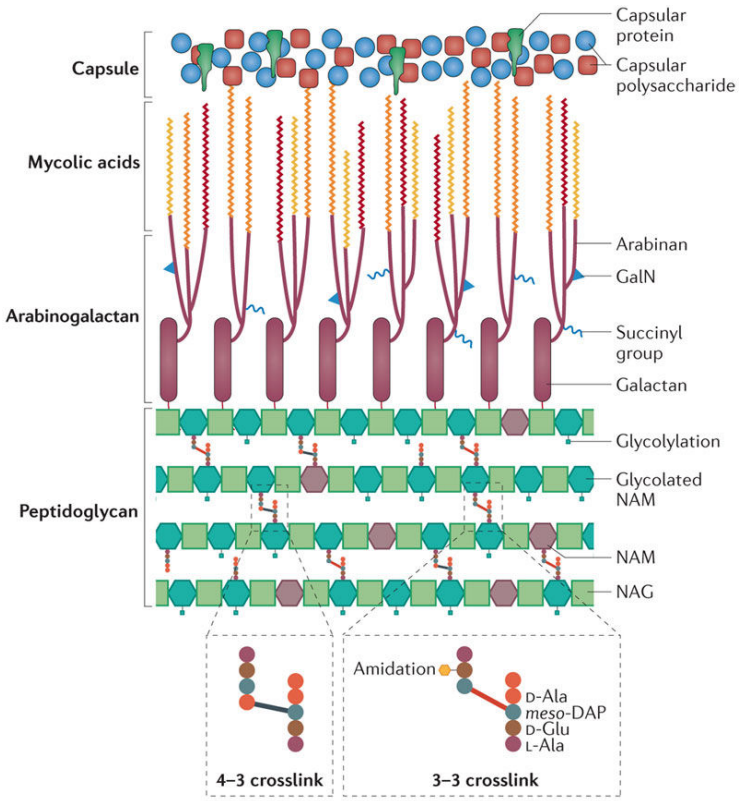


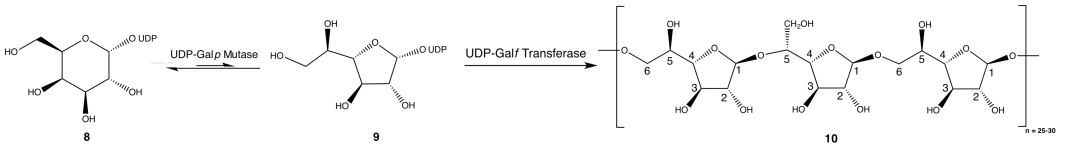
Fig. 3. Schematic showing the major component layers of the *Mycobacterial* cell wall, taken from Kieser *et al.*[57]

The peptidoglycan layer which directly surrounds the plasma membrane is composed of long repeating N-acetyl glucosamine–N-acetyl muramic acid (NAG–NAM) polymer units, connected by peptide linkages.

On top of the peptidoglycan layer is an arabinogalactan layer. This layer consists of alternating β-1,5 and β-1,6 D-galactan units which are synthesised by galactopyranose mutatase (Gal*p*M) and galactofuranosyl transferases (Gal*f*T1 and Gal*f*T2) (Scheme 2).

Most of the aforementioned galactan layer is ligated with long chain mycolic acids. It is these vicious, long chain fatty acids which give the *Mycobacterial* cell wall its characteristic thick, waxy properties. This waxy layer is a major reason for the difficulty encountered when trying to design compounds which are capable of entering the cellular environment.

Due to its intrinsic importance to the organism, the *Mycobacterium* cell wall is a common target for drug discovery campaigns. Given that these cell walls are unique to bacteria and not present in human cells, the Gal*f* biosynthetic pathway represents a 'magic bullet' target. This reflects the fact that its inhibition would not result in unwanted side effects to the host. The process of incorporating Gal*f* residues into the complex glyco polymers is a two-step pathway mediated by two enzymes, Gal*p* Mutase (Gal*p*M) and Gal*f* Transferase (Gal*f*T). In the first step UDP-Gal*p* residues undergo isomerisation to form UDP-Gal*f*. The resulting UDP-Gal*f* residues are then polymerised to form the repeating galactan structure (Scheme 2).[58]



Scheme 2. The enzymatic pathway which converts UDP-Gal*p* (8) into the polymeric Gal*f* (10) structure which makes up the TB cell wall. The isomerisation of (8) to UDP-Gal*f* (9) is carried out by the Gal*p*M. (9) is then converted to polymer (10) by Gal*f*T, the repeating cell wall units typically consist of 25-30 repeat monomers.

While the mechanism of Gl*p*M has been subject to a fair amount of investigation, the second, Gal*f*T pathway remains relatively unexplored. For this reason it represents a novel target for the development of anti-TB drugs. The Gal*f*T pathway is made up of two steps. Gal*f*T1 is responsible for the initial linkage of the first two Gal*f* molecules. Gal*f*T2 on the other hand is a polymerising glycosyltransferase which catalyses the formation of the long chain polymer, introducing the remaining 30 monosaccharides.

Iminosugars have shown their therapeutic potential through their use as glycosides inhibitors, as well as mechanistic probes. Previous work by Thomas *et al.*, has shown that iminosugars are able to act as a weak inhibitors of Gal*f*T2. This inhibition can be rationalised through inspection of the proposed transition state of the enzyme.[59]

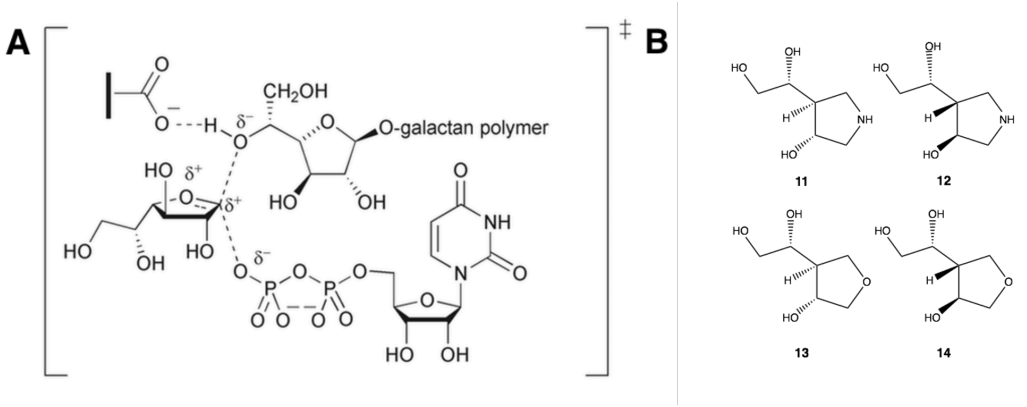


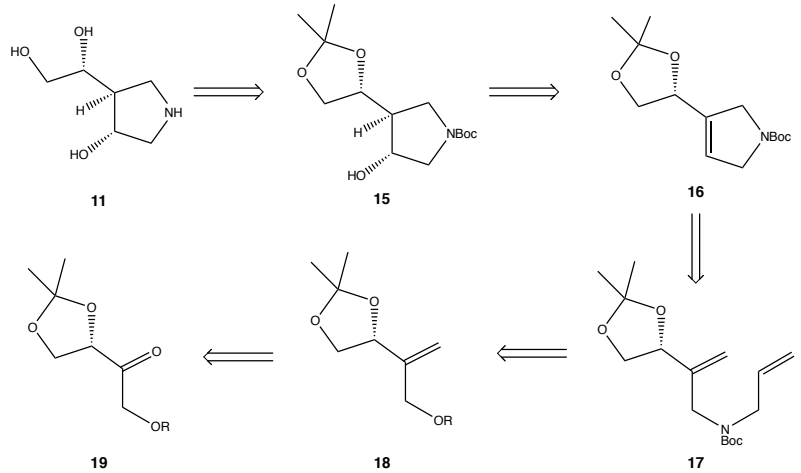
Fig 4. A) Proposed transition state for UDP-Gal*f*T enzyme substrate complex. B) Structures of four proposed inhibitors of Gal*f*T2 11-14

The postulated transition state (Fig, 4) shows how substitution of the anomeric carbon with an oxygen or a nitrogen would give a compound which could act as an inhibitor. The aim of this project is synthesise the iminosugars reported by Thomas *et al.*,[60] as well as attempting to synthesise the compounds **11** and **12**, which has not previously been reported in the literature.

Result and Discussion

A retrosynthetic analysis of target **11** is shown in scheme 2.

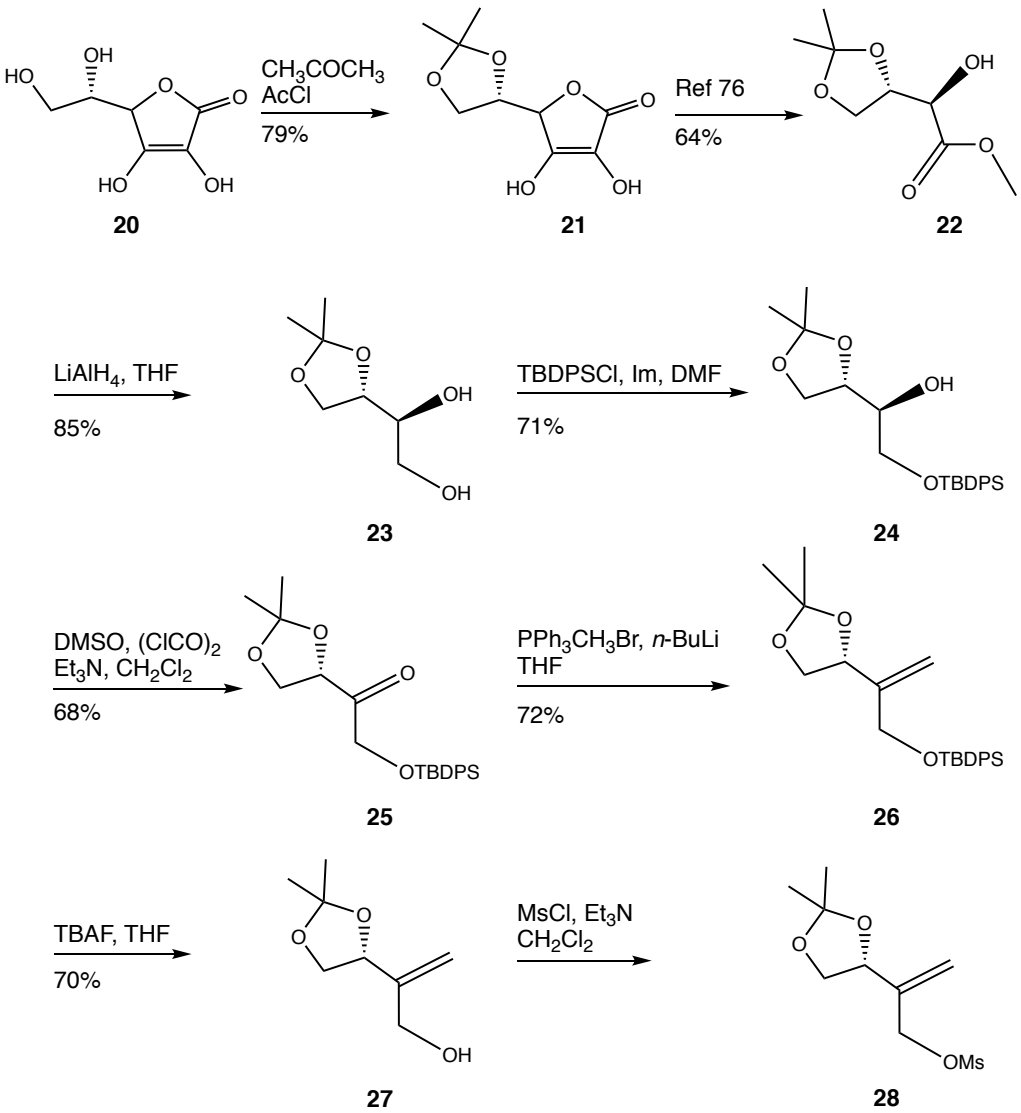
Scheme 2. Retrosynthetic analysis of Iminosugar 11



Iminosugar **11** could be unveiled through deprotection of alcohol **15**, this alcohol could be accessed by hydroboration-oxidation of alkene **16.** Alkene **16** would be obtained *via* the RCM of diene **17**. Formation of the required diene **17** would be achieved through displacement of mesylate **18** with allylamine, followed by Boc protection. Wittig chemistry would be used to convert ketone **19** into the desired alkene, which could then be converted into mesylate **18** through deprotection and mesylation of the primary alcohol.

The desired alkene structure was accessed utilising a synthesis previously reported by Abushanab *et al*. This approach utilises L-ascorbic acid (**20)** as the starting material, this is due to the fact it intrinsically possesses the desired stereochemistry for the alcohol in the 1,2 diol. (Scheme 2).[61]

Scheme 3. Construction of Mesylate 21 from L-ascorbic acid



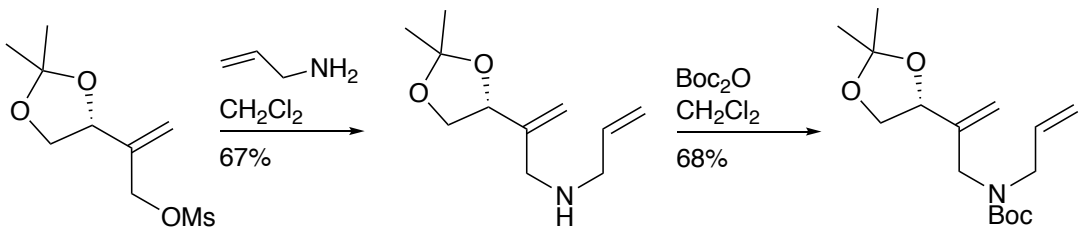
The first step of the synthesis was the protection of **20**, done using acetone and acetyl chloride, this reaction yielded the corresponding acetonide **21** in a good yield (79%). Following this, the ring structure was oxidatively cleaved with NaOH and H_2O_2, the resulting carboxylic acid was converted, *in situ*, to the corresponding methyl ester **22** using dimethyl sulfate. This was done using a method previous reported by Kim *et al.*, with an overall yield of 64%.[62] Ester **22** was then reduced using $LiAlH_4$ to give the diol **23**. In order to access ketone **25**, the primary alcohol was selectively protected using the bulky *tert*-butyldiphenylsilyl chloride (TBDPSCl) protecting group. Due to their large steric bulk, these silyl groups selectively protect primary alcohols in preference to secondary and tertiary ones. This selectivity arises

due to the steric clashes arising at the more highly substituted carbon centres. Protection of diol **23** was carried out, giving alcohol **24** in a 71% yield.

There are numerous routes to convert secondary alcohols into ketones, these include Swern, pyridinium chlorochromate (PCC) and Dess-Martin oxidation procedures.[63-65] For this synthesis, the Swern oxidation protocol was favoured due to the fact it does not generate the toxic hexavalent chromium produced during PCC oxidation and it does not require the expensive Dess-Martin periodinane (DMP) reagent. Successful oxidation of alcohol **24** gave ketone **25**. In order to access alkene **26**, a Wittig reaction was used to convert the carbonyl into an alkene, this was done using methyltriphenylphosphonium bromide. The resulting alkene **26** was then converted to allylic alcohol **27** by removal of the silyl protecting group using TBAF in order to cleave the O-Si bond. Alcohol **27** was then converted into mesylate **28** using methane sulfonyl chloride, in order to activate it as a leaving group.

Following the formation of mesylate **28**, it was necessary to introduce the second alkene component in order to create an RCM precursor (Scheme 4).

Scheme 4. Conversion of Mesylate 28 into Diene 30



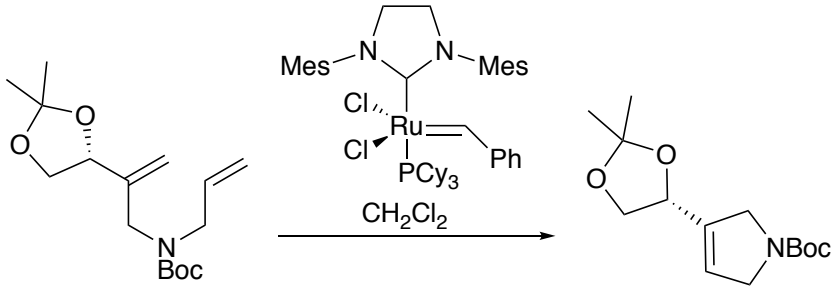
28 **29** **30**

Displacement of mesylate **28** using allylamine afforded diene **29** with a reasonable yield. In order to access the desired pyrroline structure, **31**, it was necessary to perform RCM on the diene. However, previous reports have shown that use of Grubbs catalyst with unprotected amines produces negative results as the amines coordinate to the metal centre through the lone pair, providing unwanted competing

reactions. Therefore it is necessary to add a protecting group to the amine to restrict the lone pair, so the amine was protected using Boc_2O, affording diene **30** with a 68% yield.

The use of Grubbs catalysts to perform RCM is well documented in organic synthesis and is used in the synthesis of a number of biologically active compounds. Protected diene **30** was subject to RCM using the Grubbs second generation catalyst, furnishing pyrroline **31** (Scheme 5).

Scheme 5. RCM of Diene 30 to form Pyrroline 31

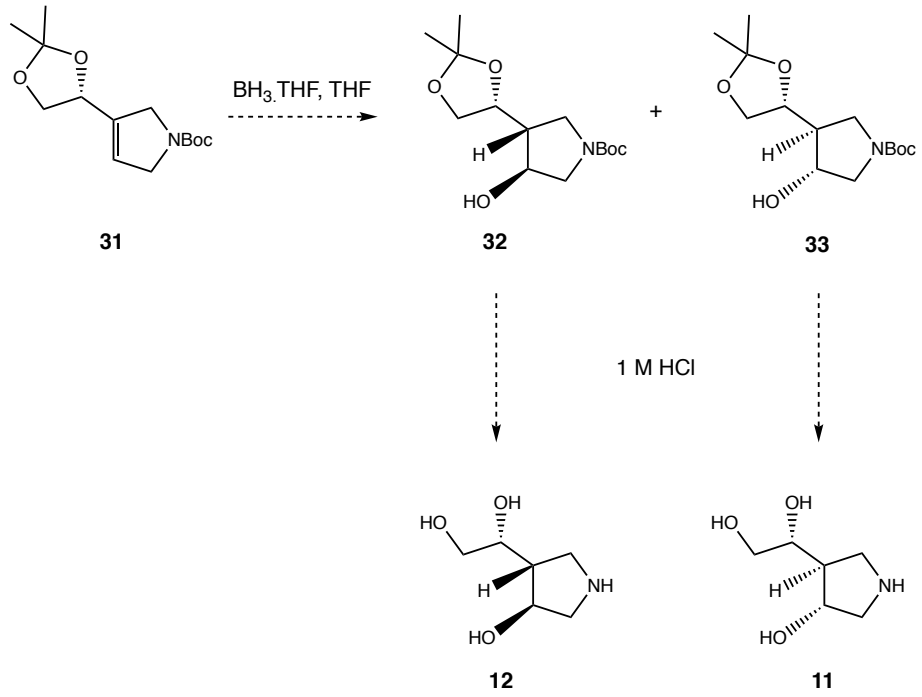


30 **31**

This reaction gave potentially positive results, with the product peak being identified *via* mass spectrometry and the formation of a new compound judged by TLC, however when the crude mixture was subject to column chromatography the product was not returned. This suggests that the product is unstable on silica and should instead be purified on an alternative stationary phase such as Florisil.

Upon successful synthesis, pyrroline **31** could then be converted into the desired iminosugars (Scheme 6).

Scheme 6. Proposed conversion of 31 into iminosugars 11 and 12

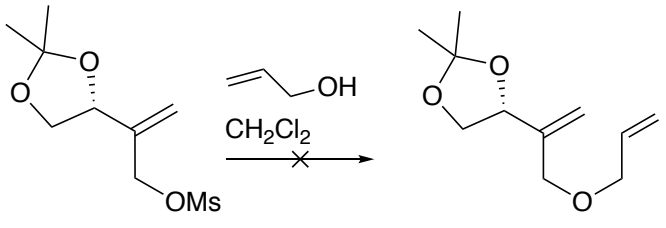


31 **32** **33** **12** **11**

Hydroboration of pyrroline **31** will yield a mix of alcohols **32** and **33** which, according to the work by Thomas *et al.,* can be separated on the basis that their polarity is different. Upon successful separation, the desired iminosugars can be accessed through deprotection of the ^{i}N-Boc and the acetal group using 1M HCl.

Given the natural substrate for Gal*f*T2 is a furanose ring, synthesis of sugars **13** and **14** was attempted using a method similar to the reported iminosugars (Scheme 7).

Scheme 7. Attempted synthesis of 34 from 28



28 **34**

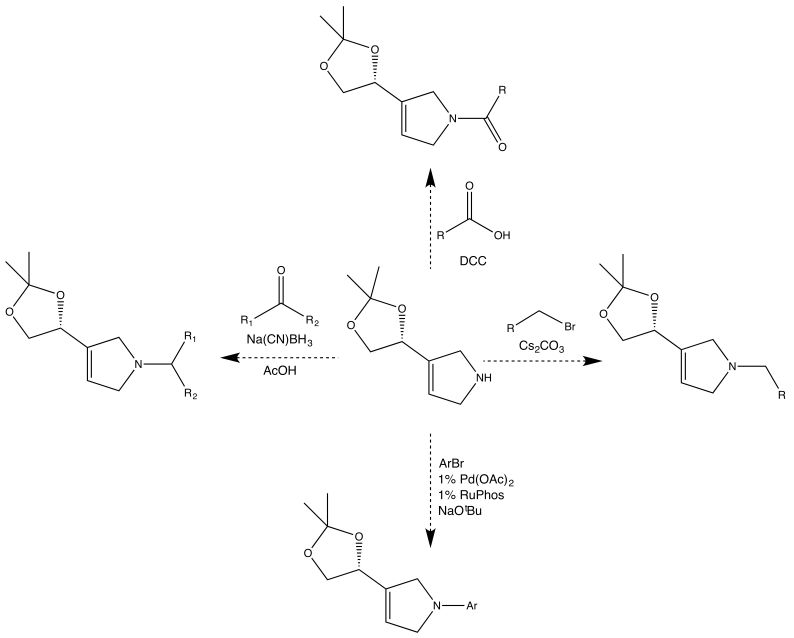
Displacement of mesylate **28** was attempted with allyl alcohol using the same conditions as performed for displacement using allyl amine. Unfortunately this

reaction did not show production of the desired product **34**. A possible explanation for this could be that allyl alcohol is a weaker nucleophile than allyl amine, owing to greater negativity of the oxygen atom compared to the nitrogen. It is possible that under more forcing conditions this displacement could be possible and would act as a way to synthesise the desired furanose moieties, which could act as novel Gal*f* inhibitors

Future Perspectives

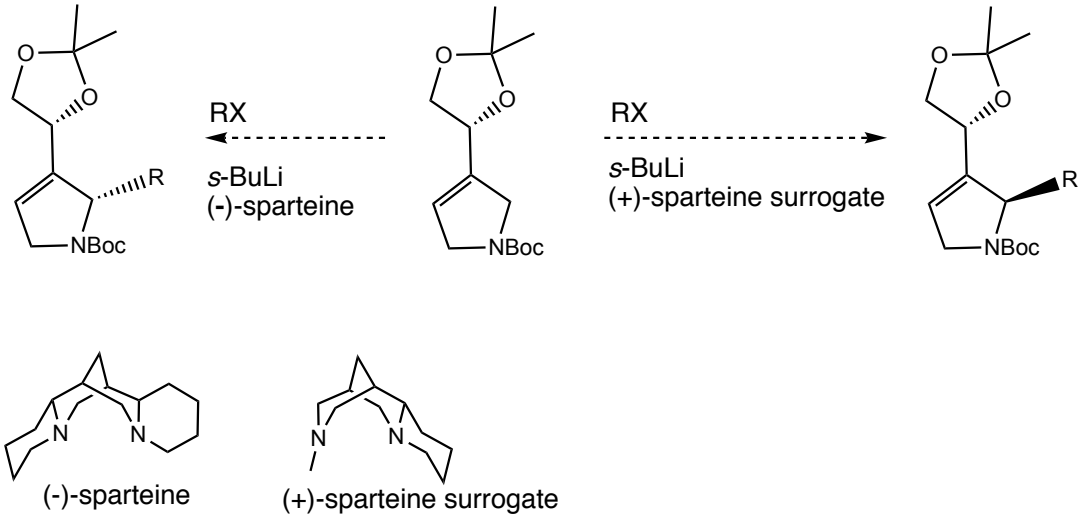
Upon synthesis of **11** it will be desirable to modify the structure in order to increase its potency as a Gal*f*T2 inhibitor. There are several potential routes for structural elaboration of the iminosugar compound class. The most obvious avenue is substitution of the amine with various functional groups to give more diverse structures. These groups would be introduced before the hydroboration step in order to ensure selectivity for the amine. Scheme 8 envisions some of the potential structures which could be synthesised from the Boc deprotected derivative of **31**, before undergoing hydroboration and deprotection to form a modified iminosugar.

Scheme 8. Proposed synthesis of iminosugars with R groups attached to the nitrogen



As well as variation of the N-R group, it is also possible to introduce new groups to the carbons α to nitrogen (Scheme 9).

Scheme 9. Proposed synthesis of derivative iminosugars using (-)-sparteine and a (+)-sparteine surrogate



Using (-)-sparteine and a (+)-sparteine surrogate, pioneered by O'Brien *et al.*, it is possible to asymmetrically deprotonate carbon atoms α to N-Boc in pyrollidine rings.[66] This approach can be used to introduce substituent groups at the α carbon, as this carbon is able to act as a nucleophile through the formation of a C-Li bond. These substituent groups could then also be subject to further modifications, expanding the scope of potential inhibitor structures.

Beyond synthetic organic chemistry, the use of *in silico* screening will play a significant role in the development of iminosugars as inhibitors of the cell wall biosynthetic pathway. As previously mentioned, the Gal*f*T2 pathway remains relatively unexplored, with a crystal structure having only recently been reported by Lowary *et al.*[67] It is envisioned that through the use of the Schrodinger software package it will be possible to use this crystal structure to map the binding site(s) within the protein.[68] This knowledge can then be used in order to lead structure based drug design of the iminosugar compound class, additionally it is possible that it could be used for more large scale virtual screening investigations to use *in*

silico docking algorithms to identify potential hit compounds from large compound libraries.

Conclusion

In summary, the direct precursor to a set of iminosugars, Gal*f*T2 inhibitors has been synthesised using a series of reactions including an RCM to access the pyrroline structure. Attempts were made to synthesis a furanose analogue of the iminosugars but initial explorations proved unsuccessful. Going forward, routes to structural elaboration have been proposed which will allow modification of the iminosugar structures in order to increase potency.

Chapter 3

CD1d-restricted NKT cells: The immune system's Swiss Army Knife

In the 1980s a unique class of T lymphocytes was identified, existing in both humans and mice.[69] These cells were seen to express the phenotypic markers found on both T and natural killer (NK) cells, so were referred to as natural killer T cells (NKT cells).[70]

The years following their identification have seen increasing interest in their biological activity and have yielded various discoveries. The existence of several antigens for NKT cells has been confirmed and there has been an increased understanding of how these antigens are recognised by receptors on the cell surface.[71]

It is the biological role of these cells which has proven their most interesting characteristic. It has been demonstrated that NKT cells play a crucial role in the regulation of many different types of immune responses. These responses include the development of self-tolerance and immune responses to pathogens and tumours.[72,73] What remains unclear is exactly how NKT cell are able to elicit such diverse responses and whether it would be possible to artificially stimulate these responses using synthetic or semi-synthetic compounds.

Unlike conventional T cells, which recognise peptide antigens on the surfaces of major histocompatibility complex (MHC) molecules, NKT cells recognise lipid antigens found on the CD1d protein from the CD1 family.[74,75] The CD1 family can be categorised into at least three different groups: group 1 contains CD1a, CD1b and CD1c; group 2 and 3 are comprised solely of CD1d and CD1e respectively.

The interaction between the receptors on the NKT cell surface and the antigen–CD1d complex represents a fundamental process leading to the activation of the NKT cell immune response. There have been numerous studies investigating the nature of antigen recognition by NKT cell receptors and how they elicit different immune responses. Although CD1d is a monomorphic, tetrameric protein, it is capable of binding to a myriad of antigens, both natural and synthetic.[76,77]

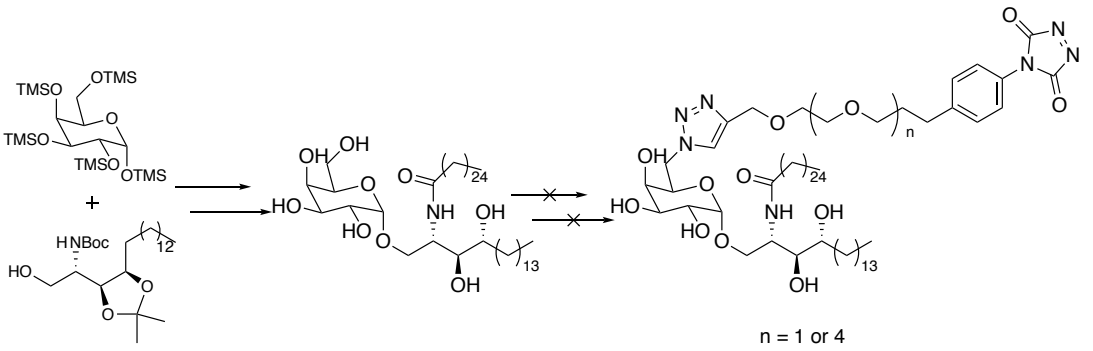
The most remarkable property of NKT cells is also the one which presents the greatest difficulty when attempting to understand and predict their actions. NKT cells are capable of eliciting such a wide range of biological responses that properly mapping the response system has, so far, confounded researchers. One of the major response systems activated by NKT cells is the rapid production of cytokines and chemokines.[78] In addition to this, NKT cells have been shown to directly kill other cells. Building upon these cytotoxic properties, NKT cells also have the ability to influence other immune cells belonging to both the innate and adaptive immune systems. These cells under influence of NKT cells include, but are not limited to, macrophages, neutrophils and dendritic cells.[79]

Broadly speaking, the major immune responses invoked by NKT cells can be categorised as T_H1 or T_H2 relating to the nature of the cytokines produced.[80,81] The T_H1 response produces anti-tumour and antimicrobial effects, whereas a T_H2 response is responsible for protection against autoimmune diseases. Given that simultaneous activation of both responses elicits an antagonistic effect, inducing a variety of unpredictable biological responses, it is important that activation of the immune response is specific. Biasing this immune response is a major goal for researchers interested in NKT cells as it could represent a new therapeutic avenue with numerous potential applications.

One of the most widely studied CD1d antigen is **KRN7000** which is a synthetic analogue of a glycosphingolipid that is derived from the Japanese marine sponge, *Agelas mauritianus*.[82-84] **KRN7000**, has been shown to bind to CD1d and elicit immuno-adjuvant properties through the further binding to the NKT cell surface receptors.

The aim of the second project reported within will focus on the synthesis of the bioactive cerebroside **KRN7000** and its 6-deoxy-6-azido analogue. **KRN7000**, also known as α-Galactosyl Ceramide (α-GalCer), has been shown to demonstrate immuno-adjuvant properties. **KRN7000** mediates its biological effects through binding to the CD1d protein. The complex formed subsequently activate NKT cells through interactions with T-cell receptors which are present on the NKT cell membranes. This activation then triggers the production of T_H1 or T_H2 cytokines. This project will look to explore the potential of NKT cell activators as an adjuvant in vaccination and whether the effectiveness of vaccines can be improved through the bioconjugation of an NKT cell activator. This conjugation will be achieved through the synthesis of a polyethylene glycol (PEG) linker, so the effect of distance between the NKT activator and the vaccine can also be explored.

Synthesis of KRN7000 and design and partial synthesis of novel azido-α-GalCer compounds containing PTAD linker motifs.

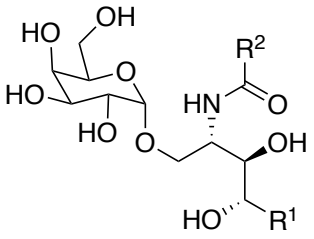


*A concise synthesis of the biologically active cerebroside compound **KRN7000** is reported. This synthesis uses a TBAI mediated glycosylation step to deliver, exclusively, the desired α-galactoside. The synthesis of an azide-containing analogue was investigated but installation of the azide functionality via a Mitsunobu reaction proved unsuccessful. Two PTAD linkers were designed which could be attached to 6-deoxy-6-azido-α-GalCer in order to investigate further conjugation to the flagellin through the PTAD moiety. A partial synthesis of these PEG compounds is reported*

Introduction

Nature is replete with incredible biological molecules and structures which have fascinated scientists from every discipline. From the unparalleled tensile strength of spider silk, to the potentially neuro-regenerative properties of snake venom, nature provides a wealth of inspiration for researchers.[85, 86] Marine sponges are no different and represent a vast resource for biologically active molecules.[87,88] Indeed, several molecules derived from marine invertebrates are currently under investigation in clinical trials.[89,90] One such interesting compound class is the cerebrosides. These compounds are glycosphingolipids and have been shown to be key components of various different tissue types as well as nerve cell membranes.[91] Glycosphingolipids are composed of two distinct structural motifs:

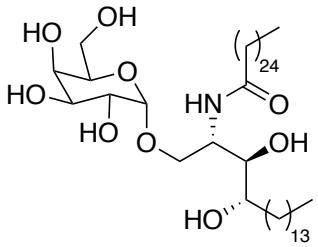
1) a ceramide unit made up of two fatty acid chains & 2) a polar, hydrophilic region, which typically comprises of a mono or polysaccharide. (Fig 5, **35**)



35

Fig 5. Structure of a generic glycosphingolipid 35

Glucosyl and galactosylceramides represent the most well studied examples of this compound class and have been widely explored over the last two decades.[92] The archetypal galactosylceramide is **KRN7000** (Fig 6, **36**)



36

Fig 6. KRN7000, 36, a galactospingolipid which has been the subject of significant research for its bio-active properties

KRN7000 is a synthetic analogue of a glycosphingolipid that is derived from the Japanese marine sponge, *Agelas mauritianus.* **KRN7000**, also known as α-GalCer, has been shown to demonstrate immuno-adjuvant properties. **KRN7000** mediates its biological effects through binding to the CD1d protein. The complex formed subsequently activate NKT cells through interactions with T-cell receptors which are present on the NKT cell membranes. This activation then triggers the production of T_H1 or T_H2 cytokines. Due to the fact the CD1d molecule must be present to trigger

these biological effects, the process is known as a CD1d-restricted response.[93] The differing responses result in the production of various other immune cells including, but not limited to, B cells and macrophages. The differing nature of the responses provide significantly different outcomes, the T_H1 response produces anti-tumour and antimicrobial effects, whereas a T_H2 response is responsible for protection against autoimmune diseases.[94] Given that simultaneous activation of both responses elicits an antagonistic effect, inducing a variety of unpredictable biological responses, it is important that activation of the immune response is specific. Attempts to improve the selectivity towards a T_H1 or a T_H2 response have yielded numerous functionalised α-GalCers (Fig 7)

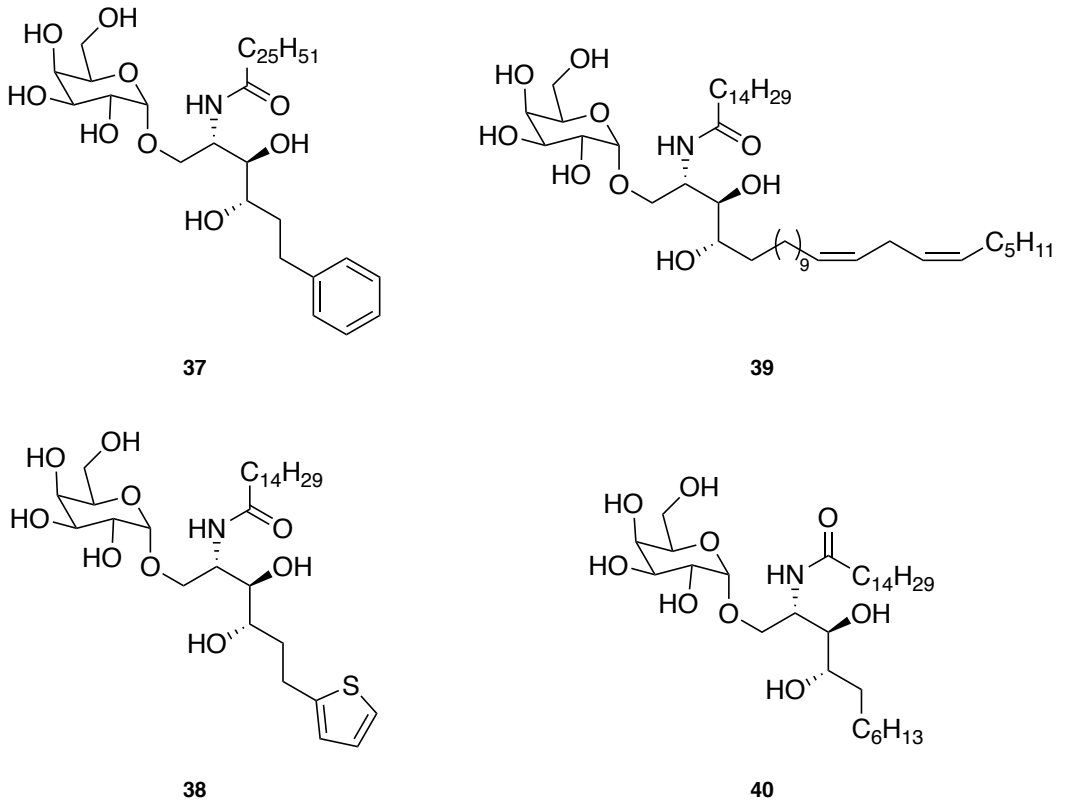


Fig 7. The structures of various galactosylceramides which show biased immune-response patterns. Compounds 37 & 38 show increased T_H1 response, whereas 39 & 40 elicit a more skewed T_H2 response

Analogues reported in the literature seem to suggest that truncation of one of the lipid chains results in a more biased T_H2 response.[83,95] The introduction of

unsaturation in the lipid chains or installation of polar groups at the C6 position of the sugar moiety also appears to direct preference towards a T_H2 response. The structures favouring a T_H1 response suggest that a rigid conformation of the spacer between the D-galactose and ceramide regions is key to accessing a T_H1 response. Other factors which appear to bias the response in favour of T_H1 are: the presence of aromatic rings or long lipid chains, the installation of a small hydrophobic molecule on the C6 sugar position or a substitution of the D-galactose moiety with a carbocyclic ring, all appear to favour a T_H1 response.[96,97]

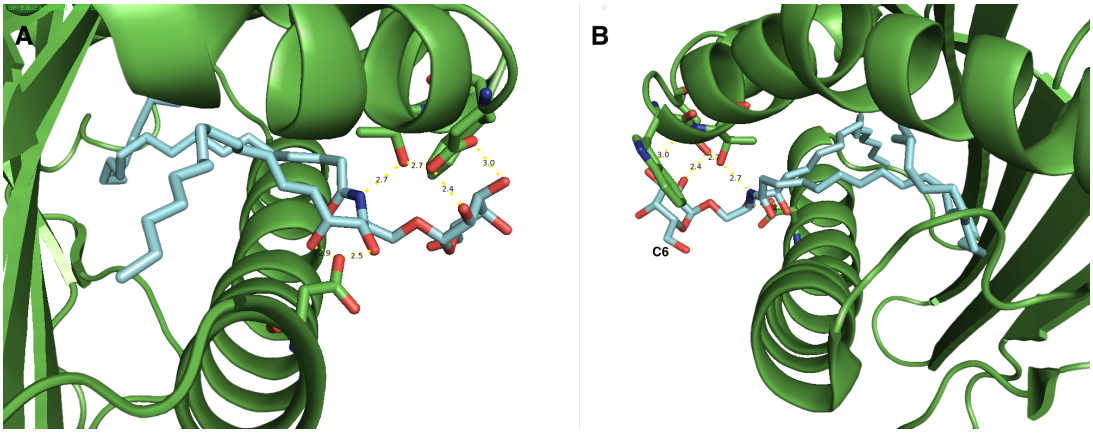


Fig 8. Crystal structure of KRN7000 bound to CD1d. This shows how the C(6)OH on the sugar moiety, highlighted in B, is not involved in the key binding interactions and so is a prime candidate for elaboration.

The crystal structure of **KRN7000** bound to CD1d shows that the C(6)OH position of the sugar moiety is not fundamental to binding, as such it represents an attractive target for functionalisation in order attempt to modulate the nature of the immune response (Fig 4).[98-100] To this end, functionalisation of the C6 position could be achieved through the introduction of an azide in place of the alcohol, this azide could then be amenable to Click Chemistry in order to introduce a range of different functionalities. One possibility is the introduction of chemical groups which allow for the bioconjugation of proteins for the preparation of vaccines, in order to afford the constituent glycoconjugate vaccine. This could be achieved

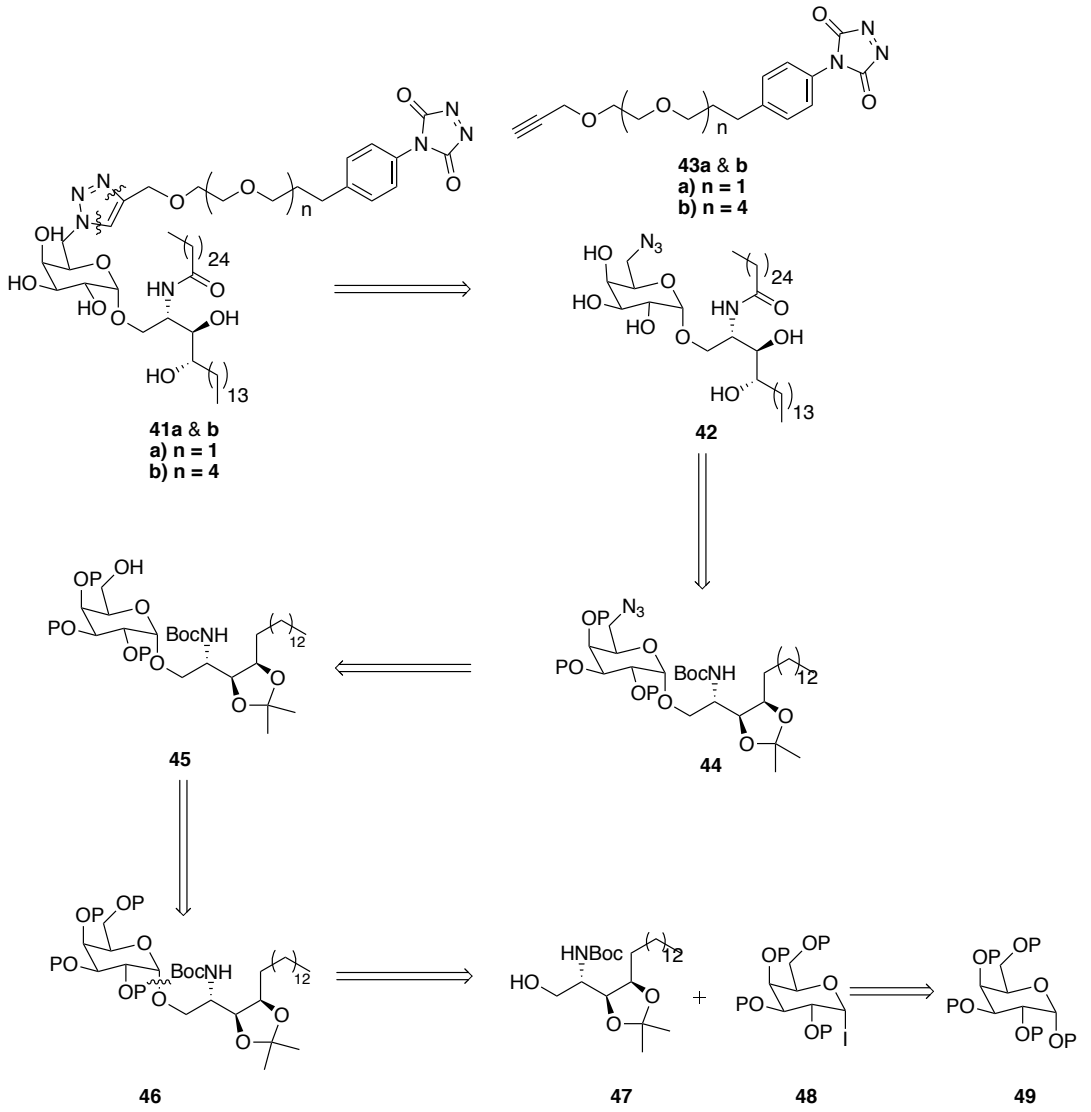
through the introduction of a 4-phenyl-1,2,4-triazole-3,5-dione (PTAD) group, which can be conjugated to a protein via a tyrosine residue. An example of this strategy has previously been reported by Hu *et al.* who conjugated an anti-candidiasis vaccine to a polysaccharide unit, through the use of PTAD-containing polyethylene glycol (PEG) linker.[101] The aim of this project is to further explore this concept and synthesise two α-GalCer derivatives with different sized PTAD-containing linkers, which will allow exploration of the potential to augment vaccine response through conjugation to a derivative of **KRN7000**.

Results and Discussion

Synthesis of KRN7000 and its corresponding azide

A retrosynthetic analysis for the target **41** is shown in Scheme 10

Scheme 10. Retrosynthetic analysis of target 41

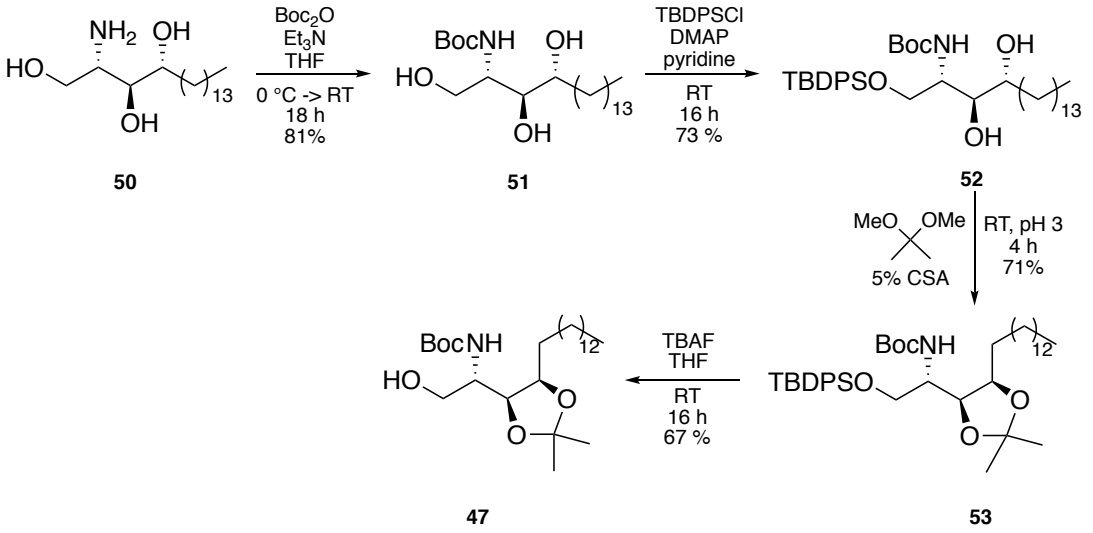


The retrosynthetic analysis of target **41** shows how the PEG linker could be installed through Click Chemistry, using traditional methods to combine **42** and **43**. Total deprotection of galactoside **44** followed by acylation of the free amine would afford the desired Click precursor **42**. The azide functionality would be introduced to the C6 position of the sugar moiety through a Mitsunobu reaction at the C6-OH on **45**. This alcohol functionality would be unveiled through the selective deprotection of the primary silyl ether on **46**. Disconnection of **46** reveals how it could be synthesised

through the glycosylation of phytosphingosine acceptor **47** and glycosyl iodide **48**, which in turn can be accessed via per silylated galactose **49**.

The synthesis of the phytosphingosine-derived glycosyl acceptor **47**, is summarised in Scheme 11.

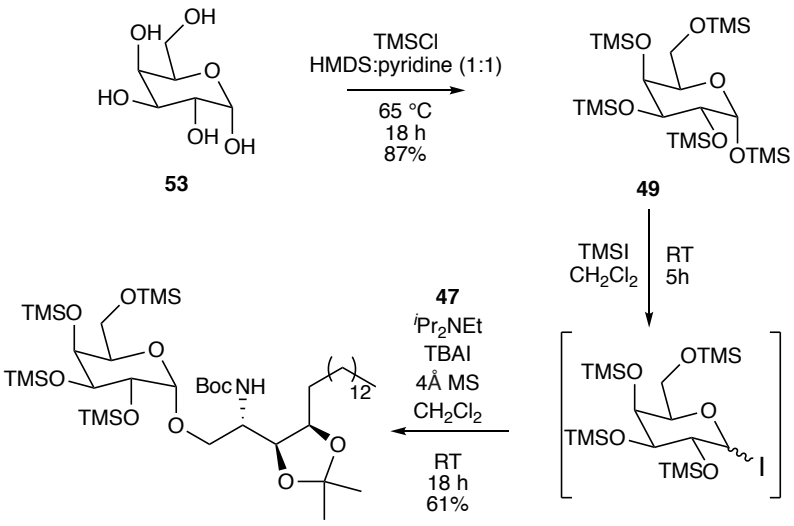
Scheme 11. Synthetic pathway to 47 starting from phytosphingosine



Initial amine protection of phytosphingosine **50** was carried out using Boc anhydride and Et_3N generating carbamate **51** in a good yield. Initial concerns that carbamate might undergo cyclisation through the neighbouring primary alcohol, to form a 5 membered 2-oxazolidone ring proved unfounded and the carbamate was obtained as the sole product. The neighbouring primary alcohol was then selectively protected as a silyl ether using TBDPSCl, pyridine in the presence of a DMAP. The large steric bulk of this silyl protection group ensure exclusive protection of primary alcohol in preference to the secondary alcohols, furnishing diol **52** in a good yield. The resulting 1,2-diol was then converted to the corresponding acetonide in order to mask these remaining alcohols. This conversion was achieved using 2,2 dimethyoxpropane and 5% camphorsulfonic acid (CSA) to afford the totally protected compound **53**. The acid catalyst was added slowly and the addition was stopped once the pH reached 3

of the reaction mixture, this was done in order to ensure the carbamate was not removed by overly acidic conditions. The totally protected compound was then subjected to selective deprotection of the primary alcohol using TBAF, affording alcohol **47** in a good yield.

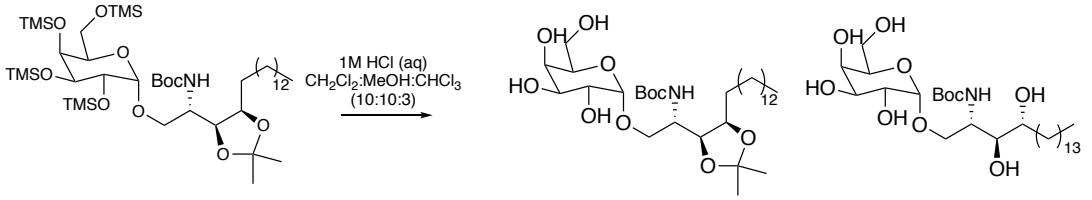
Scheme 12. Synthesis of galactoside 46.



The synthetic route to the galactoside **46** is shown in Scheme 12. Per-silylation of galactose was performed using TMSCl with a co-solvent system of HMDS and pyridine in a 1:1 ratio. This generated the desired per-silylated galactose **49** in good yield. In order convert this galactose reside to a galactosyl donor it was converted to the corresponding glycosyl iodide **48**, this was done using TMSI in CH_2Cl_2. This reactive intermediate was not isolated and was directly converted to the desired galactoside **46** via a glycosylation step. This glycosylation was performed in accordance with the method previously outlined by Gervay-Hague and Du. Due to the extreme moisture sensitivity of the iodide intermediate, the reaction was carried out in the presence of 4 Å molecular sieves (MS). Using the previously synthesised glycosyl acceptor **47**, the glycosylation reaction furnished **46** with a 61% yield, exclusively as the α configuration. This α selectivity was confirmed by measuring coupling constant of the anomeric proton, situated at 4.60 ppm in the ^{1}H NMR

spectrum. In line with the Karplus equation, the configuration of anomeric protons can be identified by their coupling constants, with a small ($^3J_{H1\text{-}H2} < 5$ Hz) coupling constant indicating α confirmation. The coupling constant observed in this instance was 3.7 Hz. Alternatively, if the glycosylation had yielded the β-glycoside, a $^3J_{H1\text{-}H2}$ value of ~ 8 - 15 Hz would be expected. This is due to the increased orbital overlap between protons with a dihedral angle of 180° which results in a larger coupling constant than those with narrower angles.

Scheme 13. Deprotection of 46 to form 55 & 56



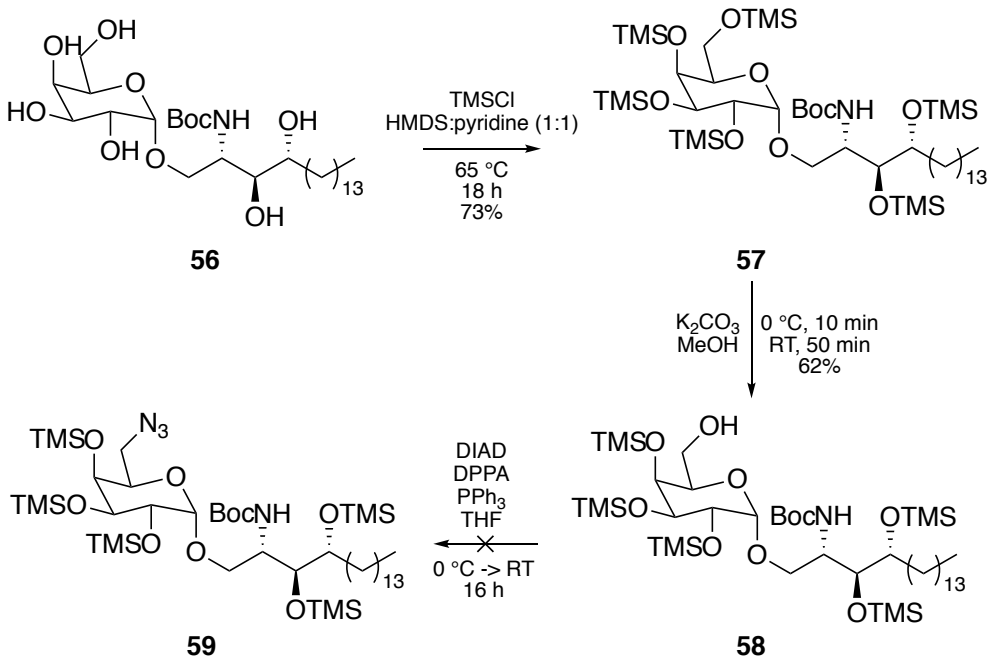
46

55
15%

56
53%

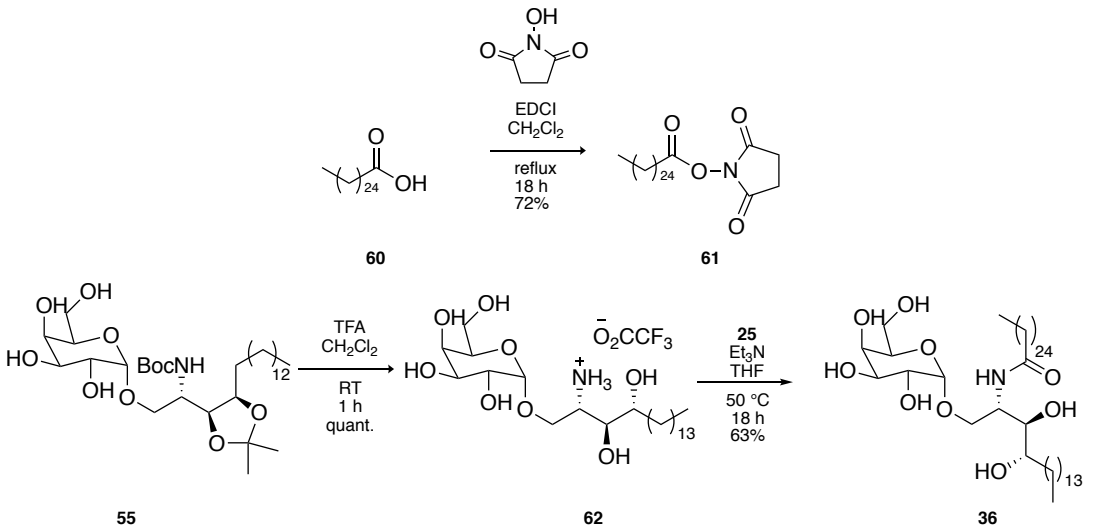
In order to purify the glycosylation product, the crude product **46** was treated with 1M HCl (aq) in a solvent system of CH_2Cl_2:MeOH:$CHCl_3$ (10:10:3), the intention being to remove the silyl protecting groups the galactose moiety, which would in turn aid separation of the product from by-products, using flash column chromatography. However, the reaction yielded a mixture of two products, the desired acetal **55**, and a second, major product, **56**, in which the acetal had also undergone hydrolysis.

Scheme 14. Attempted synthesis of Azide 59



Given that the major product of the deprotection of **46** was pentaol **56**, this compound was taken forward in order to synthesise the desired azide. Using the same protocol as previously the free alcohols were converted to their corresponding TMS ethers to provide the per-silylated galactoside **57** in a good yield. In order to unveil the C6-OH group of the galactose motif, a selective deprotection was performed using K_2CO_3 and MeOH. This reaction afforded the desired alcohol **58** in an acceptable yield with some product being lost to poly-deprotection of the peripheral TMS ethers. Conversion of the primary alcohol to azide **59** was attempted using the traditional Mitsunobu protocol, however, disappointingly this reaction proceeded slowly and attempts to isolate the suspected product were unsuccessful as this compound degraded when subjected to flash column chromatography. Despite multiple attempts, using a protocol that has been used previously in the literature, it was not possible to isolate the desired azide **59**.

Scheme 15. Conversion of Galactoside 55 to KRN7000

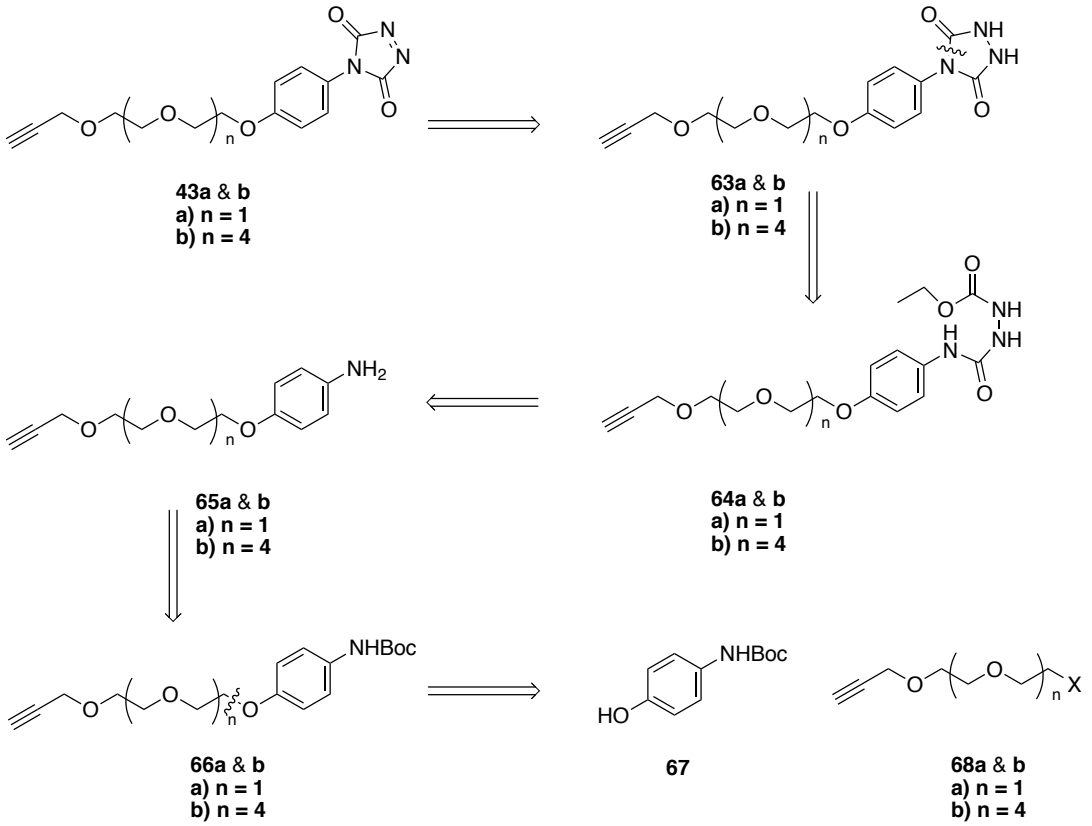


Using the acetal-protected galactoside **55** left over from the previous synthesis, **KRN7000** (**36)** was synthesised (Scheme 15). First, the remaining protecting groups were removed using TFA in CH_2Cl_2, affording the totally deprotected galactoside **62** in a quantitative yield, presumably as the TFA salt of the amine. In order to form the required C26 amide, the hexacosanoic acid **60** component was activated in the form of its NHS ester, **61**. This was prepared by treatment of the acid with *N*-hydroxsuccinimde, EDCI and CH_2Cl_2. Acylation of amine **62** was then performed using the NHS ester, in the presence of Et_3N, to afford **36** in a good yield after purification. This compound can be used as a standard in future *in vivo* experiments, in order to compare the activity of more functionalised α-GalCer-derivatives with a control.

Synthesis of the PEG linker compounds

Upon the successful synthesis of azide **59**, it will be possible to introduce the PTAD motif required for the protein bioconjugation using Click Chemistry. First, however, the corresponding alkyne containing PEG linkers must be synthesised.

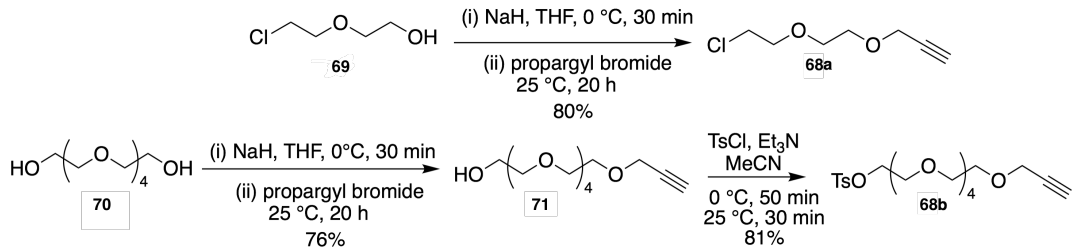
Scheme 16. Retrosynthetic analysis of targets 43 a & b



The proposed retrosynthesis for the PEG linkers is outlined in Scheme 16. The respective linkers **43 a** & **b** would be accessed through the oxidation of triazolidines **63** which in turn would be accessed through the cyclisation through the cyclisation of hydrazide-derivatives **64 a & b** under basic conditions**.** The desired hydrazide-dervatives would be formed from amines **65** using 4-nitrophenyl chloroformate and ethyl carbazate in one-pot conversion. Amines **65** would be unveiled through the Boc deprotection of carbamates **66**. Disconnection of the aromatic and PEG components unveils the readily available 4-*N*-Boc hydroxyl aniline component of the linker, **67**, and leaves two functionalised PEG components, **68**. The starting materials for the

functionalised PEG components differ. The shorter linker, **68a** can be accessed directly through the propargylation of 2-chloro-ethoxyethanol. Conversely, **68b** requires a two step functionalisation of pentaethylene glycol, first to introduce the propargyl group and secondly to activate the remaining alcohol group in the form of a tosylate. The components would then be amenable to substitution at the phenolic OH.

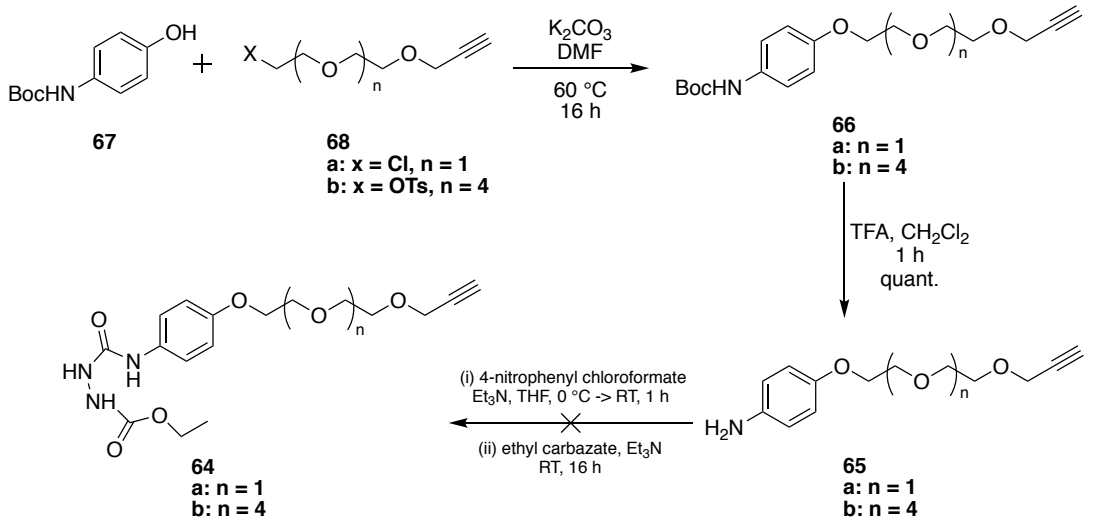
Scheme 17. Synthesis of activated PEG compounds 68a & b



The synthesis of the activated PEG compounds is shown in Scheme 17. Propargylation of both alcohol **69** and diol **70** was performed using NaH and propargyl bromide, both conversions proceeded well and in good yield. In the case of diol **70**, the diol was used in an excess, in order to avoid potential bis-propargylation. The free alcohol in alkyne **71** was then activated in the form of a tosylate, using tosyl chloride and Et_3N, affording tosylate **68b** in good yield.

The attempted synthesis of **64 a** & **b** is summarised in Scheme 18

Scheme 18. Attempted synthesis of 64a & B



Multiple strategies were investigated in order to attach the PEG groups to the protected aniline (Table 2).

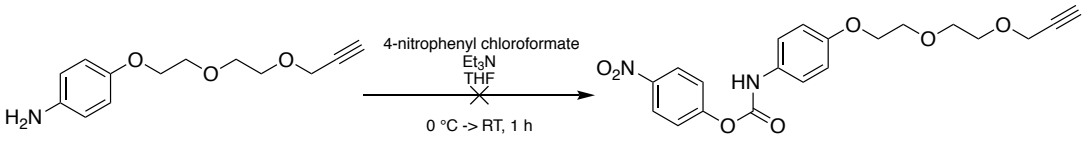
Table 2. Optimisation of the etherification of 4-*N*-Boc-aniline procedure

Solvent	Temperature / °C	Time / h	Base	Yield (**66 a**) %
MeCN	60	6	K_2CO_3	N/A
DMF	60	6	K_2CO_3	27
DMF	60	18	K_2CO_3	53

Initial attempts were carried out in accordance with work previously reported by Zheng *et al.*, the reaction mixture was heated under reflux for 6 hours in acetonitrile.[102] Unfortunately this reaction showed no formation of the desired product for either **66a** or **b**. Next, DMF was investigated as an alternate solvent system and after heating at 60 °C for 6 hours there was evidence of product formation. With this in mind, the reaction mixture was heated at 60 °C and allowed to stir for 18 hours overnight, which improved conversion and yielded the desired product in an acceptable yield. Removal of the Boc group was achieved using TFA in CH_2Cl_2 and unveiled the desired amines **65** in a quantitative yield.

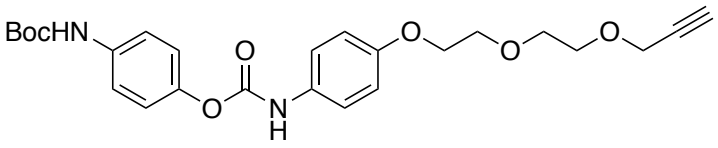
The conversion of **65 a** & **b** to **64 a** & **b** was initially attempted through a one-pot method which involved forming the corresponding carbamates, using 4-nitrophenyl chloroformate and then using these intermediates directly converted to form the desired hydrazide-derivatives. Unfortunately this reaction did not generate the desired product. The reaction produced a number of unwanted by-products and did not return detectable amounts of starting material. To remedy this issue a two-step synthesis was attempted, (Scheme 19), whereby the carbamate would be isolated before being taken forward and converted to the corresponding hydrazide-derivatives.

Scheme 19. Attempted synthesis of 72



65a **72**

In the first step of this process, a slight excess of 4-nitrophenyl chloroformate was used in the presence of an excess of Et_3N. The reaction was carried out in accordance with a published protocol which has been used to synthesise of a variety of similar carbamates, however, upon characterisation an analysis the product isolated appears to be **73**.



73

Fig 9. Structure of 73

The structure of this compound was suggested by the presence of a 9H singlet at 1.50 ppm in the ^1H NMR spectrum, corresponding to the $(CH_3)_3$ of a Boc group. An

additional peak at 28 ppm in the ^{13}C NMR spectrum, corresponding to the $C(\mathbf{C}H_3)_3$ supported the notion that the new compound contained a ^{t}Bu group. This was further supported by the fact these two resonances generated a cross peak in a HSQC NMR experiment. Additionally, the aromatic regions observed in the ^{1}H NMR spectrum were further upfield that would have been expected for the target nitrophenyl carbamate. Typically in 1,4-disubstituted nitrophenyl compounds, the hydrogens located *ortho* to the nitro group display a chemical shift of ~8.3 ppm. In **73**, the furthest downfield aromatic protons are situated at 7.5 ppm, which suggests that the neighbouring substituent is significantly less electron withdrawing than a nitro group, further supporting the idea that the NO_2 group has somehow been reduced. The mass spectrum for the isolated product showed a mass of 493 which correlates with the sodiated ion of the proposed structure.

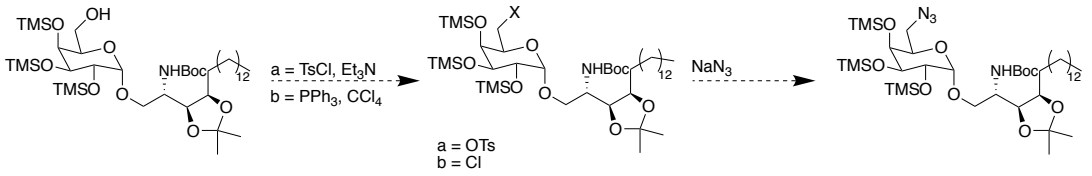
The formation of this product is particularly puzzling from two aspects, firstly the starting material was 4-nitrophenyl chloroformate, so in order for Boc protection to be possible this nitro group must first have been reduced. Reduction of nitrophenyl group requires the presence of a reducing agent, typically tin & 1M HCl (aq) or a H_2/Pd/C catalyst and typically occurs under significantly more forcing conditions than those employed during this reaction. The second issue with the formation of this product is the generation of the Boc protecting group itself, given that it was not a reagent and there is no obvious pathway for its generation through side reactions, the formation of this product remains as puzzling as its explanation is elusive.

Future Perspectives

The main synthetic problem posed by this project was the introduction of the azide group at the C6 position of the galactose moiety. Installation of this functionality is on the key step in the synthetic pathway as it will open up the molecule to Click Chemistry. With this in mind it may be necessary to investigate alternate routes to introduce the azide functionality in place of the C6-OH.

There are two obvious methods which could be used in order to achieve this conversion between functional groups. These methods are summarised in scheme 20.

Scheme 20. Possible routes for installation of azide functionality at the C6 position of the galactoside.



As opposed to the attempted Mitsunobu reaction which allows the direction conversion between alcohols and azides, the routes suggested in Scheme 20 focus on the activation of the alcohol, or its conversion to an alkyl halide. These conversions would then allow displacement of using NaN_3 in order to install the azide at the C6 position. And additional route to activating the alcohol would be in the form of a mesylate, which may provide different activity to the previously mentioned tosylate.

Conclusion

In summary, the biologically active cerebroside compound, **KRN7000**, has been synthesised through a concise method. Attempts were made to derivative to form the 6-deoxy-6-azido analogue; however, these attempts were unsuccessful. Initial work was undertaken investigating the synthesis of two different PTAD-containing PEG linkers. This synthesis proved to be problematic and is something that will require further work to refine a viable approach. Ultimately, the aim is to combine the azide and the PEG linkers through Click Chemistry and then probe how variation of the PEG linker length can augment vaccine response through conjugation to a derivative of **KRN7000.**

Concluding Remarks and Future Perspectives

While the work reported here represents a start for each of the projects discussed, there is a significant amount of work required to unlock their full potential.

Investigating the potential of iminosugars as inhibitors of TB cell biosynthesis represents a novel approach to anti-TB drugs, and as such there is significant scope for exploration. Going forward it will be necessary to express and purify the Gal*f*T2 enzyme in order to perform catalytic activity assays to explore the inhibitory properties of synthesis inhibitors. In addition to this, the natural substrate UDP-Gal*f* will need to be synthesised for use in these assays. Given that *GalfT2* is a relatively unexplored target, significant computational studies will need to be explored. These will be carried out using the published structure of the enzyme (PDB = 4FIX) and should look to explore the predicted binding modes of iminosugars to the enzyme. These binding modes could be confirmed using x-ray crystallography, if possible. Using the *in silico* predicted binding modes of the iminosugars, further computational studies could be undertaken to explore potential binding sites close to the nitrogen of the iminosugar, which would allow elaboration of the iminosugar to improve binding affinity, this approach was discussed previously. In addition to enzyme assays, whole-cell assays should be performed to test the efficacy of synthesised compounds, given the complex nature of TB's cell wall, it is often the case that compounds which are active in enzyme assays are not active *in vivo* because they are unable to pass through the complex TB cell wall. This approach will allow comprehensive exploration of the iminosugar compound class as potential anti-TB drug and could possibly identify lead compounds which could be taken forward for further investigation.

In terms of the NKT activator project. More work is required to refine the installation of the azide functionality in the synthesis of the 6-deoxy-6-azido-α-

GalCer target molecule. Alternate routes should be explored, such as conversion of the primary alcohol to a halide or mesylate, which could then be displaced using sodium azide. These alternate routes could provide a more efficient and less temperamental means to access the required azide functionality. Further work also is needed to establish an effective route to the two targeted linker compounds. Upon synthesis of the two desired compounds, it will be possible to explore their ability to augment vaccinations. For the purpose of this work, the specific vaccine modification for exploration will be anti-typhoid Vi capsular polysaccharide vaccine. This can be conjugated to the NKT cell activators through a surface tyrosine residue. The vaccine-conjugates will be delivered subcutaneously to infant mice (< 2 weeks), adult mice (8 weeks) and aged mice (18 months <) and their responses will be compared to those of mice deficient in all T cells (TCR$\beta\delta^{-/-}$) and their antigen-specific responses will be compared at 7 and 28 days after immunisation. These response can be examined in the draining lymph node, the spleen and bone marrow, these are locations where long-lived antibody responses are maintained. These examinations would be performed using an Enzyme-Linked ImmunoSpot (ELIPSOT) assay. To investigate whether the conjugation of an NKT cell activator augments the protection afforded by the vaccine, non-immunised and immunised mice will be challenged with *Salmonella Typhimurium*, which have been engineered to express the Vi antigen. After this challenge, the bacterial burdens will be assessed in the spleen, liver and bone marrow. This approach will allow a comprehensive analysis of the effects of conjugation of a vaccine with an NKT cell activator and could help significantly improve the efficacy of vaccines.

The impact and value of antibiotics cannot be overstated, in the 70 years since the introduction of penicillin we have become totally dependent on them as a means to combat infectious diseases, for this reason alone they should never be treated as simple commodities. As has been previously mentioned, antibiotics have uses beyond therapeutics for infected individuals, they have been critical to the

successful expansion of advanced surgical procedures most importantly organ transplants. The spectre of rapidly emerging AMR bacteria threatens the render the extraordinary use of these drugs meaningless.[103]

Far from a localised issue, this a global crisis and one which reflects the worldwide overuse of these drugs and also big pharma's failure to properly invest in the development of new antibiotics.[104] The O'Neill review highlighted just how enormous the clinical and financial burden on health care systems is, as well as the significant damage to wider global economy.

In the era of 'fake news', where we're told that the public is 'sick of experts' it is more important than ever that the scientific community does not let-up on the issue of AMR.[105-107] More must be done in the government lobby chambers, as well as scientific laboratories, to ensure those in positions of power are aware of just how real the dangers of AMR. There are no simple solutions to this problem and in order to successfully address the crisis of AMR there must be a coordinated, global, effort to implement new policies and establish new research programmes. Given that the severity of AMR is akin to that of climate change, it seems strange there is, as of yet, no international treaty designed to create a global solution to AMR, in the way that The Paris Accord does for climate change. However, any such treaty would require unilateral implementation and given the increasingly fractured nature of international relations, it is difficult to envision such a treaty being negotiated in the very near future. Decisive actions that require significant commitment and stringent enforcement are rarely popular, but the issue of AMR is one that transcends politics and is one that must be tackled head-on before it is too late.

It would be naive to think that there is a perfect antibiotic, because this simply is not the case. However, once new compounds are identified and their use cases are established, it is essential that prescription of these antibiotic be restricted to those uses. It may be the case that new antibiotics must be treated as 'controlled substances' in order to properly manage their usage. It is likely that this will result in the emergence of 'niche' antibiotics which should be treated as a separate classes, distinct from the broad-spectrum antibiotics. Given the increases in diagnostic tools and the knowledge of environmental reservoirs of resistance, surveillance should start to play an increasingly significant role in the fight against AMR. This will make it possible to have early warnings of potential resistance mechanisms to antibiotics and thus allow those in clinical settings to proactively prepare for such issues, as well as triggering research from pharmaceutical companies into means to overcome new resistance mechanisms. It is the duty of the scientific community to take full advantage of the increased understanding and new technologies at our disposal in order to renew a concerted offensive against AMR.[108,109] There is no single group of people who, alone, can effectively fight the war on AMR, it will take broad collaboration from politicians, scientists, clinicians and agriculturalists, as well as the compliance of the general public in order to turn the tide.

As Alexander Fleming oversaw the transition from the *pre-antibiotic era* into a *golden age*, his warnings of the potential ramifications of unabated antibiotic use were not heeded and now humanity must work to correct these failings, if not, the *post-antibiotic era* awaits our descendants.

References

(1) Miller, E. L. *J. Midwifery Women's Health* **2002**, 47, 426.

(2) Silver, L. L. *Clin. Microbiol. Rev.* **2011**, 24, 71.

(3) Wohlleben, W.; Mast, Y.; Stegmann, E.; Ziemert, N. *Microb. Biotechnol.* **2016**, *9*, 541.

(4) Hampson, F. G.; Ridgway, E. J. *Surgery - Oxford International Edition*, 23, 293.

(5) Davies, J.; Davies, D. *Microbiol Mol Biol Rev* **2010**, *74*, 417.

(6) Blair, J. M. A.; Webber, M. A.; Baylay, A. J.; Ogbolu, D. O.; Piddock, L. J. V. *Nat Rev Micro* **2015**, *13*, 42.

(7) Chaudhary, A. S. *Acta Pharma. Sin. B* **2016**, 6, 552.

(8) McArthur, A. G.; Waglechner, N.; Nizam, F.; Yan, A.; Azad, M. A.; Baylay, A. J.; Bhullar, K.; Canova, M. J.; De Pascale, G.; Ejim, L.; Kalan, L.; King, A. M.; Koteva, K.; Morar, M.; Mulvey, M. R.; O'Brien, J. S.; Pawlowski, A. C.; Piddock, L. J. V.; Spanogiannopoulos, P.; Sutherland, A. D.; Tang, I.; Taylor, P. L.; Thaker, M.; Wang, W.; Yan, M.; Yu, T.; Wright, G. D. *Antimicrob. Agents Chemother.* **2013**, *57*, 3348.

(9) "The Review on Antimicrobial Resistance.". Final Report. http://amr-review.org/Publications (Accessed July 17th 2017)

(10) Wise, E. M.; Abou-Donia, M. M. *Proc Natl Acad Sci U S A* **1975**, *72*, 2621.

(11) Skold, O. *Antimicrob. Agents Chemother.* **2000**, 3, 155.

(12) Byrne-Bailey, K. G.; Gaze, W. H.; Kay, P.; Boxall, A. B. A.; Hawkey, P. M.; Wellington, E. M. H. *Antimicrob. Agents Chemother.* **2009**, *53*, 696.

(13) Zaman, S. B., *9*.

(14) Tan, S. Y.; Tatsumura, Y. *Singapore Med. J.* **2015**, *56*, 366.

(15) Winkle, W. V.; Herwick, R. P. *J. Am. Pharm. Assoc.* **1945**, 34, 97.

(16) Flemming, A. 1945; Vol. 2017.

(17) Lewis, K. Nat. *Rev. Drug Discov* **2013**, 12, 371.

(18) Ventola, C. L. *P & T,* **2015**, 40, 277.

(19) Sakula, A. *Can. Vet. J.* **1983**, 24, 127.

(20) Raviglione, M.; Sulis, G. *Curr. Infect. Dis. Rep.* **2016**, *8*.

(21) Bunyasi, E. W.; Schmidt, B.-M.; Abdullahi, L. H.; Mulenga, H.; Tameris, M.; Luabeya, A.; Shenje, J.; Scriba, T.; Geldenhuys, H.; Wood, R.; Hatherill, M. *BMJ Open* **2017**, *7*.

(22) Beggs, C. B.; Noakes, C. J.; Sleigh, P. A.; Fletcher, L. A.; Siddiqi, K. *Int. J. Tuberc. Lung Dis*., **2003**, 7, 1015.

(23) Pawlowski, A.; Jansson, M.; Sköld, M.; Rottenberg, M. E.; Källenius, G. *PLOS Pathogens* **2012**, *8*, e1002464.

(24) Manosuthi, W.; Wiboonchutikul, S.; Sungkanuparph, S. *AIDS Res. Ther.* **2016**, *13*, 22.

(25) Gelband, H. *Cochrane Database Syst Rev* **2000**, Cd001362.

(26) Horsburgh, C. R.; Barry, C. E.; Lange, C. *N Engl J Med* **2015**, *373*.

(27) Koul, A.; Arnoult, E.; Lounis, N.; Guillemont, J.; Andries, K. *Nature* **2011**, *469*, 483.

(28) Walker, D.; Stevens, W. *Expert Opin. Pharmacother.,* **2003**, 4, 359.

(29) Volmink, J. *PLoS Med*.

(30) Jin, J.; Sklar, G. E.; Min Sen Oh, V.; Chuen Li, S. *Ther. Clin. Risk Manag.* **2008**, *4*, 269.

(31) Castelnuovo, B. *Afr Health Sci.,* **2010**, 10, 320.

(32) Sharma, S. K.; Kaushik, G.; Jha, B.; George, N.; Arora, S.; Gupta, D.; Singh, U.; Hanif, M.; Vashisht, R. *Indian J. Med. Res.* **2011**, *133*, 308.

(33) Mekonnen, F.; Tessema, B.; Moges, F.; Gelaw, A.; Eshetie, S.; Kumera, G. *BMC Infect Dis* **2015**, *15*.

(34) Caminero, J. A.; Sotgiu, G.; Zumla, A.; Migliori, G. B. *Lancet Infect Dis* **2010**, *10*, 621.

(35) Pinto, L.; Menzies, D. *Infect. Drug Resist.* **2011**, *4*, 129.

(36) Timmins, G. S.; Deretic, V. *Mol. Microbiol.* **2006**, *62*, 1220.

(37) Cade, C. E.; Dlouhy, A. C.; Medzihradszky, K. F.; Salas-Castillo, S. P.; Ghiladi, R. A. *Protein Sci.,* **2010**, *19*, 458.

(38) Tseng, S.-T.; Tai, C.-H.; Li, C.-R.; Lin, C.-F.; Shi, Z.-Y. *J. Microbiol. Immunol. Infect.* **2015**, *48*, 249.

(39) van Ingen, J.; Aarnoutse, R. E.; Donald, P. R.; Diacon, A. H.; Dawson, R.; Plemper van Balen, G.; Gillespie, S. H.; Boeree, M. J. *Clin. Infect. Dis.* **2011**, *52*, e194.

(40) Norton, B. L.; Holland, D. P. *Infect. Drug Resist.* **2012**, *5*, 163.

(41) Almeida Da Silva, P. E.; Palomino, J. C. *J. Antimicrob. Chemother.* **2011**, *66*, 1417.

(42) De La Iglesia, A. I.; Morbidoni, H. R. *Rev. Argent. Microbiol.* **2006**, *38*, 97.

(43) Gunther, G. *Clin. Med.* **2014**, 14, 279.

(44) Chan, E. D.; Iseman, M. D. *Curr. Opin. Infect. Dis.* **2008**, 21, 587.

(45) Velayati, A. A.; Farnia, P.; Masjedi, M. R. *Int. J. Clin. Exp. Med.* **2013**, 6, 307.

(46) Khan, F. A.; Minion, J.; Pai, M.; Royce, S.; Burman, W.; Harries, A. D.; Menzies, D. *Clin. Infect. Dis.* **2010**, *50*, 1288.

(47) Mahatthanatrakul, W.; Nontaput, T.; Ridtitid, W.; Wongnawa, M.; Sunbhanich, M. *J. Clin. Pharma. Therap.* **2007**, *32*, 161.

(48) Bolt, H. M. *Drug Metab. Rev.* **2004**, 36, 497.

(49) Berendonk, T. U.; Manaia, C. M.; Merlin, C.; Fatta-Kassinos, D.; Cytryn, E.; Walsh, F.; Burgmann, H.; Sorum, H.; Norstrom, M.; Pons, M. N.; Kreuzinger, N.; Huovinen, P.; Stefani, S.; Schwartz, T.; Kisand, V.; Baquero, F.; Martinez, J. L. *Nature Rev. Microbiol.* **2015**, *13*, 310.

(50) Mullard, A. *Nat. Rev. Drug Discov.* **2016**, 15, 663.

(51) .

(52) Russell, D. G. *Nat. Rev. Mol. Cell Biol.* **2001**, 2, 569.

(53) Stewart, G. R.; Robertson, B. D.; Young, D. B. *Nat Rev. Microbiol.* **2003**, *1*, 97.

(54) Maxmen, A. *Nature* **2013**, *502*, S4.

(55) Ma, Y.; Stern, R. J.; Scherman, M. S.; Vissa, V. D.; Yan, W.; Jones, V. C.; Zhang, F.; Franzblau, S. G.; Lewis, W. H.; McNeil, M. R. *Antimicrob. Agents Chemother.* **2001**, *45*, 1407.

(56) Sanders, D. A.; Staines, A. G.; McMahon, S. A.; McNeil, M. R.; Whitfield, C.; Naismith, J. H. *Nat. Struct. Mol. Biol* **2001**, *8*, 858.

(57) Kieser, K. J.; Rubin, E. J. *Nat. Rev. Microbiol* **2014**, *12*, 550.

(58) Breton, C.; Snajdrova, L.; Jeanneau, C.; Koca, J.; Imberty, A. *Glycobiology* **2006**, *16*, 29r.

(59) Cren, S.; Gurcha, S. S.; Blake, A. J.; Besra, G. S.; Thomas, N. R. *Org. Biomol. Chem.* **2004**, *2*, 2418.

(60) Cren, S.; Wilson, C.; Thomas, N. R. *Org. Lett.* **2005**, *7*, 3521.

(61) Abushanab, E.; Bessodes, M.; Antonakis, K. *Tetrahedron Lett.* **1984**, *25*, 3841.

(62) Cho, B. H.; Kim, J. H.; Jeon, H. B.; Kim, K. S. *Tetrahedron* **2005**, *61*, 4341.

(63) Corey, E. J.; Suggs, J. W. *Tetrahedron Lett.* **1975**, *16*, 2647.

(64) Omura, K.; Sharma, A. K.; Swern, D. *J. Org. Chem.* **1976**, *41*, 957.

(65) Dess, D. B.; Martin, J. C. *J. Org. Chem* **1983**, *48*, 4155.

(66) Dearden, M. J.; Firkin, C. R.; Hermet, J.-P. R.; O'Brien, P. *J. Am. Chem. Soc.* **2002**, *124*, 11870.

(67) Wheatley, R. W.; Zheng, R. B.; Richards, M. R.; Lowary, T. L.; Ng, K. K. S. *J. Bio. Chem.* **2012**, *287*, 28132.

(68) Halgren, T. A. *J. Chem. Inf. Model* **2009**, 49, 377.

(69) Godfrey, D. I.; MacDonald, H. R.; Kronenberg, M.; Smyth, M. J.; Kaer, L. V. *Nat Rev Immunol* **2004**, *4*, 231.

(70) Taniguchi, M.; Harada, M.; Dashtsoodol, N.; Kojo, S. *Proc. Jpn. Acad., Ser B Phys. Biol. Sci* **2015**, 91, 292.

(71) Godfrey, D. I.; McCluskey, J.; Rossjohn, J. *Nature Immunol.* **2005**, *6*, 754.

(72) Kronenberg, M.; Gapin, L. *Nat Rev Immunol* **2002**, *2*, 557.

(73) Godfrey, D. I.; Stankovic, S.; Baxter, A. G. *Nature Immuno* **2010**, *11*, 197.

(74) Blumberg, R. S.; Gerdes, D.; Chott, A.; Porcelli, S. A.; Balk, S. P. *Immunol. Rev.* **1995**, *147*, 5.

(75) Cohen, N. R.; Garg, S.; Brenner, M. B. *Adv. Immunol.* **2009**, *102*, 1.

(76) Brutkiewicz, R. R. *J. immunol.* **2006**, 177, 769.

(77) Rossjohn, J.; Pellicci, D. G.; Patel, O.; Gapin, L.; Godfrey, D. I. *Nat Rev Immunol* **2012**, *12*, 845.

(78) Coquet, J. M.; Chakravarti, S.; Kyparissoudis, K.; McNab, F. W.; Pitt, L. A.; McKenzie, B. S.; Berzins, S. P.; Smyth, M. J.; Godfrey, D. I. *Proc. Nat. Acad. Sci. U.S.A.* **2008**, *105*, 11287.

(79) Matsuda, J. L.; Mallevaey, T.; Scott-Browne, J.; Gapin, L. *Curr. Opin. Immunol.* **2008**, *20*, 358.

(80) Onoe, K.; Yanagawa, Y.; Minami, K.; Iijima, N.; Iwabuchi, K. *Immunol. Res.,* **2007**, *38*, 319.

(81) Ru, W.; Peijie, C. *Int. J. Biol. Sci*. **2009**, 5, 338.

(82) Sullivan, B. A.; Kronenberg, M. *J. Clin. Invest.* **2005**, *115*, 2328.

(83) Yu, K. O. A.; Im, J. S.; Molano, A.; Dutronc, Y.; Illarionov, P. A.; Forestier, C.; Fujiwara, N.; Arias, I.; Miyake, S.; Yamamura, T.; Chang, Y.-T.; Besra, G. S.; Porcelli, S. A. *Proc. Nat. Acad. Sci. U.S.A.* **2005**, *102*, 3383.

(84) Park, J. J.; Lee, J. H.; Ghosh, S. C.; Bricard, G.; Venkataswamy, M. M.; Porcelli, S. A.; Chung, S. K. *Bioorg Med Chem Lett* **2008**, *18*, 3906.

(85) Chin, T. Y.; Kiat, S. S.; Faizul, H. G.; Wu, W.; Abdullah, J. M. *The Malays. J. Med. Sci.* **2017**, *24*, 31.

(86) Harvey, D.; Bardelang, P.; Goodacre, S. L.; Cockayne, A.; Thomas, N. R. *Adv. Mat.* **2017**, *29*, n/a.

(87) Simmons, T. L.; Andrianasolo, E.; McPhail, K.; Flatt, P.; Gerwick, W. H. *Mol. Cancer Ther.* **2005**, *4*, 333.

(88) Blunt, J. W.; Copp, B. R.; Keyzers, R. A.; Munro, M. H. G.; Prinsep, M. R. *Nat. Prod. Rep.* **2016**, *33*, 382.

(89) Newman, D. J.; Cragg, G. M. *Curr. Med. Chem.* **2004**, *11*, 1693.

(90) Newman, D. J.; Cragg, G. M. *J. Nat. Prod.* **2004**, *67*, 1216.

(91) Tan, R. X.; Chen, J. H. *Nat Prod Rep* **2003**, *20*, 509.

(92) Yu, K. O.; Porcelli, S. A. *Immunol. Lett.* **2005**, *100*, 42.

(93) Morita, M.; Motoki, K.; Akimoto, K.; Natori, T.; Sakai, T.; Sawa, E.; Yamaji, K.; Koezuka, Y.; Kobayashi, E.; Fukushima, H. *J. Med. Chem.* **1995**, *38*, 2176.

(94) Biosci., Biotech., and Biochem. **1996**, 60, 288.

(95) Velmourougane, G.; Raju, R.; Bricard, G.; Im, J. S.; Besra, G. S.; Porcelli, S. A.; Howell, A. R. *Bioorg. Med. Chem. Lett.* **2009**, *19*, 3386.

(96) Fujio, M.; Wu, D.; Garcia-Navarro, R.; Ho, D. D.; Tsuji, M.; Wong, C.-H. *J. Am. Chem. Soc.* **2006**, *128*, 9022.

(97) Chang, Y.-J.; Huang, J.-R.; Tsai, Y.-C.; Hung, J.-T.; Wu, D.; Fujio, M.; Wong, C.-H.; Yu, A. L. *Proc. Nat. Acad. Sci. U.S.A.* **2007**, *104*, 10299.

(98) Koch, M.; Stronge, V. S.; Shepherd, D.; Gadola, S. D.; Mathew, B.; Ritter, G.; Fersht, A. R.; Besra, G. S.; Schmidt, R. R.; Jones, E. Y.; Cerundolo, V. *Nature Immunol.* **2005**, *6*, 819.

(99) Hénon, E.; Dauchez, M.; Haudrechy, A.; Banchet, A. *Tetrahedron* **2008**, *64*, 9480.

(100) Nadas, J.; Li, C.; Wang, P. G. *J. Chem. Inf. Model.* **2009**, 49, 410.

(101) Hu, Q.-Y.; Allan, M.; Adamo, R.; Quinn, D.; Zhai, H.; Wu, G.; Clark, K.; Zhou, J.; Ortiz, S.; Wang, B.; Danieli, E.; Crotti, S.; Tontini, M.; Brogioni, G.; Berti, F. *Chem. Sci.* **2013**, *4*, 3827.

(102) Song, S.; Zheng, H.-F.; Li, D.-M.; Wang, J.-H.; Feng, H.-T.; Zhu, Z.-H.; Chen, Y.-C.; Zheng, Y.-S. *Org. Lett.* **2014**, *16*, 2170.

(103) Boucher, H. W.; Talbot, G. H.; Bradley, J. S.; Edwards, J. E.; Gilbert, D.; Rice, L. B.; Scheld, M.; Spellberg, B.; Bartlett, J. Clin. infect. Dis. **2009**, *48*, 1.

(104) Power, E. Clin. *Microbiol. Infect.* **2006**, 12, 25.

(105) Milman, O. S., D. Carrington, D.; The Guardian: 2017; Vol. 2017.

(106) Sun, L. H.; The Washington Post: 2017; Vol. 2017.

(107) Yuhas, A.; The Guardian: 2017; Vol. 2017.

(108) Baltz, R. H. J. Indust. Microbiol. Biotechnol. **2006**, 33, 507.

(109) Payne, D. J.; Gwynn, M. N.; Holmes, D. J.; Pompliano, D. L. *Nat. Rev.. Drug Discov* **2007**, *6*, 29.

Supplementary Information

General Experimental 56

Experimental Procedure for Targeting TB: Development of new inhibitors of *Mycobacterium tuberculosis* galactofuranosyl transferase Gal*f*T2 58

Experimental Procedure for Synthesis of **KRN7000** and design and partial synthesis of novel azido-α-GalCer compounds containing PTAD linker motifs. 69

General Experimental

^{1}H NMR and ^{13}C NMR spectra were recorded in $CDCl_3$ unless specified otherwise, at 400 and 100 MHz, or 300 and 75 MHz, respectively. Chemical shifts are reported as δ values (ppm) referenced to the following solvent signals: $CHCl_3$, δ_H 7.26; $CDCl_3$, δ_C 77.0; CH_3OD, δ_H 3.34; CD_3OD, δ_C 49.9. The term, 'stack' is used to describe a region where resonances arising from non-equivalent nuclei are coincident, and multiplet, m, to describe a region where resonances arising from a single nucleus (or equivalent nuclei) are coincident but coupling constants cannot be readily assigned. Connectivities were deduced from COSY90, HSQC and HMBC experiments. Mass spectra were recorded on a liquid chromatography time-of-flight (LCT) spectrometer utilizing electrospray ionization with a methanol mobile phase and are reported as (*m/z* (%)). HRMS were recorded on a LCT spectrometer using a lock mass incorporated into the mobile phase.

Reactions were monitored by thin layer chromatography using pre-coated glass-backed silica plates (60A F_{254}) and visualized by UV detection (at 254 nm) or by staining with ammonium molybdate(IV) - cerium(IV) sulfate staining dip, or 5% phosphomolybdic acid in EtOH (MPA spray), or 1% α-naphthol, 5% H_2SO_4 in EtOH. Column chromatography was performed on silica gel (particle size 40–63 μm mesh).

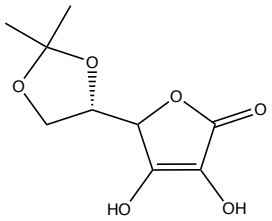
All reactions were conducted in oven-dried (140 °C) or flame-dried glassware under a nitrogen atmosphere, and at ambient temperature (20 to 25 °C) unless specified otherwise, with magnetic stirring. Volumes of 1 mL or less were measured and dispensed with gastight syringes. Evaporation and

concentration under reduced pressure was performed at 50–500 mbar at 40 °C. Residual solvent was removed under high vacuum (1 mbar).

All reagents were obtained from commercial sources and used without further purification unless specified otherwise.

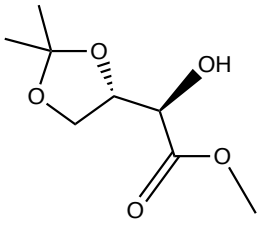
Experimental Procedure for Targeting TB: Development of new inhibitors of *Mycobacterium tuberculosis* galactofuranosyl transferase Gal*f*T2

5-((*S*)-2,2-dimethyl-1,3-dioxolan-4-yl)-3,4-dihydroxyfuran-2(5*H*)-one (21)



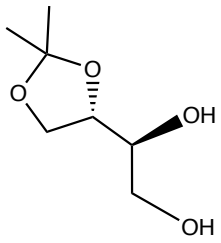
L-ascorbic acid, **20**, (5.00 g, 28 mmol) was mechanically stirred in acetone (60 mL). Acetyl chloride (2.50 mL) was added and the solution was stirred for 2 h at 40 °C. The resulting solid was cooled to −10 °C before being filtered and washed with cold acetone and then dried under reduced pressure, affording acetonide **21** as a white solid (4.81 g, 79%) The product was used without further purification: *Rf* = 0.2 (EtOAc); δ_H (300 MHz, D_2O) 1.39 (s, 6H), 4.19 (dd, *J* = 9.1, 5.0 Hz, 1H), 4.33 (dd, *J* = 9.0, 7.3 Hz, 1H), 4.61 (ddd, *J* = 7.2, 5.1, 2.2 Hz, 1H), 4.93 (d, *J* = 2.2 Hz, 1H); δ_C (101 MHz, D_2O) δ_C, 26.5, 27.3, 67.6, 75.5, 78.5, 113.3, 120.0, 159.7, 176.3; HRMS (ESI) *m*/*z* calcd for $C_9H_{12}NaO_6$ $[M + Na]^+$ 239.0526, found 239.0526 ($[M + Na]^+$, 100%)

methyl (*R*)-2-((*S*)-2,2-dimethyl-1,3-dioxolan-4-yl)-2-hydroxyacetate (22)



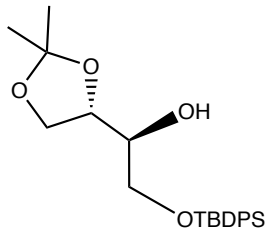
Acetonide **21** (4.81 g, 22.20 mmol) was dissolved in H_2O (25 mL). 30% NaOH (1.70 mL) was added dropwise over 5 min, the resulting solution turned clear. $NaHCO_3$ (4.70 g, 55.94 mmol) was added to this clear solution, followed by dropwise addition of 35% H_2O_2 (4.33 mL, 44.40 mmol). The resulting solution was stirred for 1 h at 20 °C. Sodium sulfite (0.33 g, 2.65 mmol) and $NaHCO_3$ (2.80 g, 33.30 mmol) were added and the reaction mixture was heated to 40 °C, followed by dropwise addition of dimethyl sulfate (5.52 mL, 88.82 mmol) over 5 min, the reaction mixture was then stirred for 4 h at 40 °C. The solution was then allowed to cool to room temperature before CH_2Cl_2 (50 mL) was added and the aqueous phase was successively extracted with CH_2Cl_2 (3 × 50 mL). The combined organic layers were dried ($MgSO_4$), filtered and concentrated under reduced pressure giving **22** as a colourless oil (2.69 g, 64%): *Rf* = 0.6 (EtOAc); ^{1}H NMR (400 MHz, $CDCl_3$) δ 1.35 (s, 3H), 1.42 (s, 3H), 3.00 (s, 1H), 3.82 (s, 3H), 4.15 – 3.95 (m, 3H), 4.39 (td, *J* = 6.8, 2.8 Hz, 1H); ^{13}C NMR (101 MHz, $CDCl_3$) δ_C 25.3, 26.0, 52.7, 65.6, 70.3, 76.3, 110.0, 172.5; HRMS (ESI) *m*/*z* calcd for $C_8H_{14}NaO_5$ $[M + Na]^+$ 213.0733, found 213.0740 ($[M + Na]^+$, 100%)

(*S*)-1-((*S*)-2,2-dimethyl-1,3-dioxolan-4-yl)ethane-1,2-diol (23)



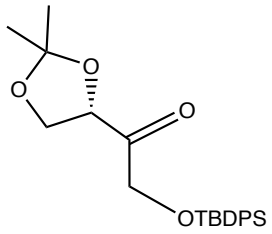
Ester **22** (2.69 g, 15.24 mmol) was dissolved in anhydrous THF (25 mL), $LiAlH_4$ (2.4 M in THF, 8.30 ml, 19.81 mmol) was added dropwise to the solution at 0 °C (ice bath). The resulting solution was stirred overnight at 20 °C. The reaction was quenched by careful addition of H_2O (6 mL) which resulted in the formation of a white precipitate. The solution was filtered through celite and washed with ethyl acetate (50 mL). The filtrate was concentrated under reduced pressure to afford diol **23** as a colourless oil (2.12 g, 85%): *Rf* = 0.3 (EtOAc); δ_H (400 MHz, $CDCl_3$) 1.44 (s, 3H), 2.86 (s, 1H), 3.03 (s, 1H), 3.72 – 3.58 (m, 3H), 3.84 (dd, *J* = 8.3, 6.7 Hz, 1H), 4.04 (dd, *J* = 8.3, 6.6 Hz, 1H), 4.17 (td, *J* = 6.6, 4.8 Hz, 1H); δ_C (101 MHz, $CDCl_3$) 25.3, 26.4, 64.0, 65.82, 71.9, 76.6, 109.6; HRMS (ESI) *m/z* calcd for $C_7H_{14}NaO_4$ $[M + Na]^+$ 185.0790, found 185.0785 ($[M + Na]^+$, 100%)

(*S*)-2-((*tert*-butyldiphenylsilyl)oxy)-1-((*S*)-2,2-dimethyl-1,3-dioxolan-4-yl)ethan-1-ol (24)



Diol **23** (2.12 g, 12.95 mmol) was dissolved in anhydrous DMF (30 mL). Imidazole (1.76 g, 25.89 mmol) was added to the solution at 20 °C, followed by *tert*-butyldiphenylsilyl chloride (3.36 mL, 12.94 mmol), this resulted in the formation of a pale yellow solution which was then stirred overnight. H_2O (30 mL) and Et_2O (50 mL) were added, the resulting layers were then separated. The isolated aqueous layer was extracted with Et_2O (3 × 50 mL). The organic layers were then combined and dried ($MgSO_4$), filtered and concentrated under reduced pressure. The crude oil was purified by column chromatography (petroleum ether (40-60):diethyl ether, 2:1), affording **24** as a colourless oil (3.68 g, 71%): *Rf* = 0.3 (petroleum ether (40-60):diethyl ether, 2:1); δ_H (400 MHz, $CDCl_3$) 1.07 (s, 9H), 1.38 (s, 3H), 1.42 (s, 3H), 2.44 (s, 1H), 3.75 – 3.63 (m, 3H), 3.82 (dd, *J* = 8.2, 7.0 Hz, 1H), 4.00 (dd, *J* = 8.2, 6.5 Hz, 1H), 4.22 (ddd, *J* = 6.9, 4.6 Hz, 1H), 7.70 – 7.35 (m, 10H); δ_C (101 MHz, $CDCl_3$) 19.2, 25.4, 26.5, 26.9, 65.0, 66.0, 71.9, 76.4, 109.2, 127.8, 129.9, 133.0, 135.6; HRMS (ESI) *m/z* required for $C_{23}H_{32}NaO_4Si$ $[M + Na]^+$ 423.1968, found 423.1962 ($[M + Na]^+$, 100%) calcd for $C_{26}H_{37}N_2O_4Si$ $[M + C_3H_5N_2]^+$ 469.2517, found 469.2519 ($[M + C_3H_5N_2]^+$, 42%)

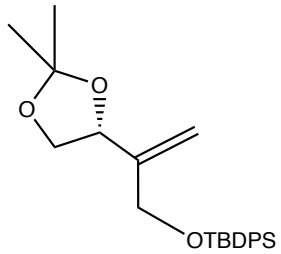
(*S*)-2-((*tert*-butyldiphenylsilyl)oxy)-1-(2,2-dimethyl-1,3-dioxolan-4-yl)ethan-1-one (25)



Oxalyl chloride (1.61 ml, 18.42 mmol) was dissolved in anhydrous CH_2Cl_2 (40 mL) and cooled to –60 °C, DMSO (2.63 ml, 37.00 mmol) was added dropwise to the solution at –60 °C, the resulting solution was stirred for 5 min before dropwise addition of alcohol **24** (3.68 g, 9.24 mmol) in CH_2Cl_2 (20 mL) such that the temperature was maintained at –60 °C. The solution formed a white suspension which was stirred for 15 min before the addition of Et_3N (5.15 mL, 37.00 mmol). The resulting pale yellow suspension was allowed to warm to 0 °C over 1.5 h. The resulting yellow suspension was diluted by the addition of CH_2Cl_2 (30 mL) and H_2O (30 mL). The aqueous layer was then extracted with CH_2Cl_2 (3 × 50 mL). The combined organic layers were dried ($MgSO_4$), filtered and concentrated under reduced pressure. The crude oil was purified by column chromatography (petroleum ether (40-60):diethyl ether, 2:1). Ketone **25** was obtained as a colourless oil (2.51 g, 68%): *Rf* = 0.5 (petroleum ether (40-60):diethyl ether, 2:1); δ_H (400 MHz, $CDCl_3$) δ 1.11 (s, 9H), 1.33 (s, 3H), 3.88 (dd, *J* = 8.8, 5.6 Hz, 1H),1.36 (s, 3H), 4.21 (dd, *J* = 8.7, 7.9 Hz, 1H), 4.55 (s, 2H), 4.62 (dd, *J* = 7.9, 5.6 Hz, 1H), 7.78 – 7.38 (m, 10H); δ_C (101 MHz, $CDCl_3$) 19.1, 25.0, 25.7, 26.6, 66.3, 68.0, 78.9, 111.0, 127.7, 129.6, 134.9, 135.6, 207.2; HRMS (ESI) *m/z* calcd for $C_{23}H_{30}NaO_4Si$ $[M + Na]^+$ 421.1811, found

421.1816 ([M + Na]$^+$, 100%), calcd for $C_{26}H_{35}N_2O_4Si$ [M + $C_3H_5N_2$]$^+$ 467.2361, found 467.2364 ([M + $C_3H_5N_2$]$^+$, 53%)

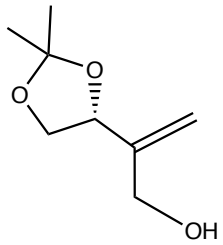
(*R*)-*tert*-butyl((2-(2,2-dimethyl-1,3-dioxolan-4-yl)allyl)oxy)diphenylsilane (26)



Ph_3PCH_3Br (3.16 g, 8.85 mmol) was dissolved in dry THF (50 mL). n-BuLi (2.4 M in THF, 2.90 mL, 6.94 mmol) was added dropwise at 0 °C. The resulting bright yellow suspension was stirred at 20 °C for 3 h. Ketone **25** (2.51 g, 6.32 mmol) was dissolved dry THF (20 mL) and then added at –78 °C. The resulting orange suspension was stirred at –78 °C for 45 min, then at 20 °C for 2 h. The reaction was quenched by dropwise addition of MeOH (10 mL) at 0 °C. Et_2O (100 mL) was added and the organic phase was successively washed with saturated aqueous NH_4Cl (3 × 100 mL) and saturated aqueous NaCl (3 × 100 mL). The combined aqueous layers were back-extracted with diethyl ether (3 × 200 mL). The combined organic extracts were dried ($MgSO_4$), filtered and concentrated under reduced pressure. The crude residue was purified by column chromatography (hexane:diethyl ether, 10:1). Alkene **26** was obtained as a colourless oil (1.78 g, 72%): *Rf* = 0.3 (hexane:diethyl ether, 10:1); δ_H (400 MHz, $CDCl_3$) 1.11 (s, 9H), 1.41 (s, 6H), 3.67 (app. t, *J* = 8 Hz, 1H), 4.16 (dd, *J* = 8.2, 6.5 Hz, 1H), 4.23 (d, *J* = 0.8 Hz, 1H), 4.67 – 4.58 (m, 1H), 5.33 – 5.27 (m, 2H), 7.79 – 7.37 (m, 10H); δ_C (101 MHz, $CDCl_3$) 19.0, 22.7, 26.6, 31.6, 64.3, 69.5, 76.8, 109.0, 111.0, 127.7,

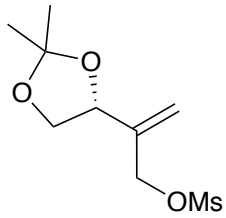
129.7, 134.8, 135.5, 145.7; HRMS (ESI) *m/z* calcd for $C_{24}H_{32}NaO_3Si$ [M + Na]$^+$ 419.2018, found 419.2012 ([M + Na]$^+$, 100%)

(*R*)-2-(2,2-dimethyl-1,3-dioxolan-4-yl)prop-2-en-1-ol (27)



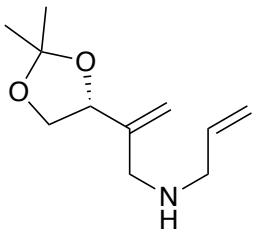
Alkene **26** (1.78 mg, 4.54 mmol) was dissolved in dry THF (20 mL). TBAF (1.0 M in THF, 9.64 mL, 9.64 mmol) was added dropwise and the resulting yellow solution was stirred at 20 °C for 24 h. The reaction was quenched using saturated aqueous NH_4Cl (20 mL), the layers were separated and the aqueous layer was washed with diethyl ether (3 × 30 mL). The combined organic extracts were dried ($MgSO_4$), filtered and concentrated under reduced pressure. The crude oil was purified by column chromatography (diethyl ether) and **27** was obtained as a colourless oil (509 mg, 70%): *Rf* = 0.7 (diethyl ether); δ_H (400 MHz, $CDCl_3$) 1.40 (s, 3H), 1.46 (s, 3H), 2.57 (bs, 1H), 3.70 (dd, *J* = 8.3, 7.1 Hz 1H), 4.13 (dd, *J* = 8.3, 6.6 Hz, 1H), 4.20 (d, *J* = 13.2 Hz, 1H), 4.66 (app. t, *J* = 7.1 Hz, 1H), 5.23 – 5.16 (m, 2H); δ_C (101 MHz, $CDCl_3$) 25.5, 26.6, 63.4, 68.9, 77.8, 109.5, 113.7, 143.3; HRMS (ESI) *m/z* calcd for $C_8H_{14}NaO_3$ [M + Na]$^+$ 181.0841, found 181.0817 ([M + Na]$^+$, 100%)

(*R*)-2-(2,2-dimethyl-1,3-dioxolan-4-yl)allyl methanesulfonate (28)



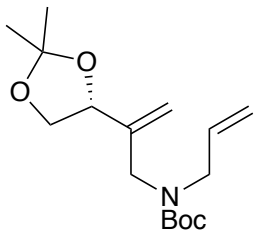
Alcohol **27** (509 mg, 3.22 mmol) was dissolved in CH_2Cl_2 (20 mL). Et_3N (2.76, 4.82 mmol) was added at 0 °C, followed by methanesulfonyl chloride (0.39 mL, 4.82 mmol). The resulting colourless solution was stirred at 0 °C for 1 h. The reaction was quenched by addition of H_2O (10 mL) and the layers separated. The organic layer was extracted with 1M HCl (20 mL), saturated aqueous $NaHCO_3$ (20 mL) and H_2O (20 mL). The organic layer was then dried ($MgSO_4$), filtered and concentrated under reduced pressure to yield **28** as a colourless oil which was used without any purification: *Rf* = 0.1 (hexane:diethyl ether, 1:1); δ_H (400 MHz, $CDCl_3$) 1.42 (s, 3H), 1.47 (s, 3H), 3.03 (s, 3H), 3.75 (dd, *J* = 8.4, 7.4 Hz, 1H), 4.20 (dd, *J* = 8.3, 6.5 Hz, 1H), 4.66 (app. t, *J* = 7.0 Hz, 1H), 4.82 – 4.75 (m, 2H), 5.40 (bs, 1H), 5.48 (bs, 1H); δ_C (101 MHz, $CDCl_3$) 26.5, 26.6, 37.9, 68.8, 69.1, 76.5, 109.7, 117.7, 140.0; HRMS (ESI) *m/z* required for $C_9H_{16}NaO_5S$ $[M + Na]^+$ 259.0616, found 259.0615 ($[M + Na]^+$, 100%)

(*R*)-*N*-allyl-2-(2,2-dimethyl-1,3-dioxolan-4-yl)prop-2-en-1-amine (29)



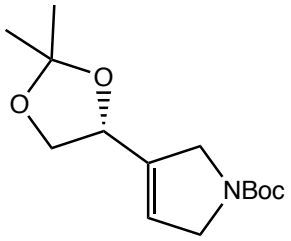
Mesylate **28** (536 mg, 2.78 mmol) in CH_2Cl_2 (10 mL) was slowly added to a stirred solution of allylamine (0.85 mL, 11.38 mmol) in CH_2Cl_2 (20 mL). The resulting colourless solution was stirred at 20 °C for 24 h. The mixture was then concentrated under reduced pressure and the residue purified by column chromatography (petroleum ether (40-60):diethyl ether, 1:2, 0.5% NH_3). Amine **29** was obtained as a yellow liquid (300 mg, 67%): *Rf* = 0.4 (petroleum ether (40-60):diethyl ether, 1:2, 0.5% NH_3); δ_H (400 MHz, $CDCl_3$) 1.41 (2 × s, 3H), 1.46 (2 × s, 3H), 3.19 - 3.40 (m, 4H), 4.15 (dd, *J* = 8.1, 6.6 Hz, 1H), 4.67 – 4.58 (m, 1H), 5.30 - 5.09 (m, 4H), 5.97 (ddt, *J* = 16.1, 10.5, 5.8 Hz, 1H); δ_C (101 MHz, $CDCl_3$) 26.6, 26.7, 53.4 (resonance overlap), 65.9, 78.0, 109.4, 112.8, 117.0, 118.7, 136.8 145.1; HRMS (ESI) *m/z* calcd for $C_{11}H_{20}NO_2$ [M + Na]$^+$ 198.1489, found 198.1497 ([M + H]$^+$, 100%)

***tert*-butyl (*R*)-allyl(2-(2,2-dimethyl-1,3-dioxolan-4-yl)allyl)carbamate (30)**



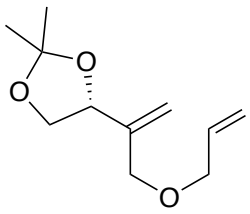
Amine **29** (300 mg, 1.52 mmol) was dissolved in n-hexane (10 mL). A solution of Di-*tert*-butyl dicarbonate (332 mg, 1.52 mmol) in *n*-hexane (5 mL) was then added dropwise at 0 °C, and the resulting colourless solution was stirred at 20 °C for 1 h. A solution of 0.01 N HCl (20 mL) was then added, the layers separated and the organic layer washed with saturated aqueous $NaHCO_3$ (20 mL), dried ($MgSO_4$), filtered and concentrated under reduced pressure to give a crude oil. The residue was purified by column chromatography (hexane:diethyl ether, 3:1) and diene **30** was obtained as a yellow oil (308 mg, 68%): *Rf* = 0.4 (hexane:diethyl ether, 3:1); δ_H (400 MHz, $CDCl_3$) 1.39 (s, 9H), 1.40 (s, 3H), 3.58 (app t, *J* = 6.3 Hz, 1H), 3.73 – 3.63 (m, 4H), 4.10 – 4.03 (m, 2H), 4.49 (app. t, *J* = 6.7 Hz, 1H), 5.28 – 4.89 (m, 4H), 5.77 (ddt, *J* = 17.1, 10.6, 5.4 Hz, 1H); δ_C (101 MHz, $CDCl_3$) 26.60, 28.3, 43.1, 43.2, 63.4, 76.8, 79.3, 114.6, 115.5, 137.7, 142.6, 155.9; HRMS (ESI) *m/z* calcd for $C_{16}H_{27}NNaO_4$ $[M + Na]^+$ 320.1838, found 320.1829 ($[M+Na]^+$, 100%)

***tert*-butyl (*R*)-3-(2,2-dimethyl-1,3-dioxolan-4-yl)-2,5-dihydro-1*H*-pyrrole-1-carboxylate (31)**



Diene **30** (308 mg, 1.04 mmol) was dissolved in dry CH_2Cl_2 (40 mL). Ruthenium catalyst (10 mg, 1 mol%) was added in 3 portions at 20 °C. The resulting purple solution turned brown after 10 min. The reaction mixture was stirred at 20 °C for 36 h, and then concentrated under reduced pressure: *Rf* 0.22 (n-hexane/diethyl ether, 2:1). HRMS (ESI) *m*/*z* required for $C_{17}H_{28}N_3O_4$ $[M + C_3H_5N_2]^+$ 338.2074, found 338.2061 ($[M + C_3H_5N_2]^+$, 100%)

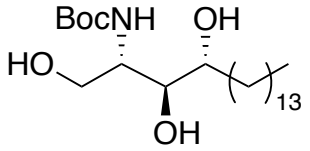
(*R*)-4-(3-(allyloxy)prop-1-en-2-yl)-2,2-dimethyl-1,3-dioxolane (34)



Mesylate **28** (300 mg, 1.56 mmol) in CH_2Cl_2 (10 mL) was slowly added to a stirred solution of allyl alcohol (0.45 mL, 6.36 mmol) in CH_2Cl_2 (20 mL). The resulting colourless solution was stirred at 20 °C for 24 h. The mixture was then concentrated under reduced pressure to give a crude yellow oil.

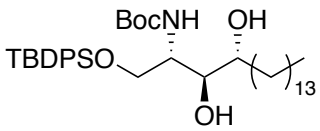
Experimental Procedure for Synthesis of KRN7000 and design and partial synthesis of novel azido-α-GalCer compounds containing PTAD linker motifs.

***tert*-butyl ((2*S*,3*S*,4*R*)-1,3,4-trihydroxyoctadecan-2-yl)carbamate (51)**



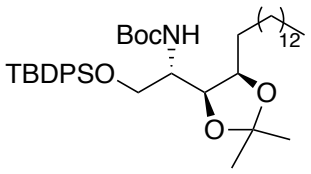
Et_3N (4.40 mL, 31.5 mmol) and Boc_2O (4.12 g, 18.9 mmol) were added sequentially to a vigorously stirred suspension of phytosphingosine (5.00 g, 15.8 mmol) in THF (100 mL). After 18 h, the reaction mixture was concentrated under reduced pressure. Recrystallisation of the residue from EtOAc (200 mL) yielded carbamate **51** as white crystals (5.32 g, 81%): *Rf* = 0.5 (hexane:EtOAc 1:1); δ_H ($CDCl_3$, 300 MHz) 0.87 (t, *J* = 6.9 Hz, 3H), 1.19-1.37 (stack, 22H), 1.44 (s, 9H), 1.44-1.76 (stack, 4H), 3.11 (bs, OH) 3.59-3.75 (stack, 3H), 3.76-3.92 (stack, 2H), 5.43 (d, *J* = 7.8 Hz, 1H), Only one O*H* resonance observed; δ_C ($CDCl_3$, 100 MHz) 14.1, 22.7, 25.9, [28.4, 29.3, 29.6, 29.7, 31.9, 33.1, resonance overlap], 53.0, 62.0, 72.9, 76.9, 80.1, 156.5; LR-MS (TOF ES+) *m*/*z* calcd for $C_{23}H_{47}NNaO_5$ $[M + Na]^+$ 440.3, found 440.3 ($[M + Na]^+$, 100%).

tert-butyl ((2_S_,3_S_,4_R_)-1-((_tert_-butyldiphenylsilyl)oxy)-3,4-dihydroxyoctadecan-2-yl)carbamate (52)



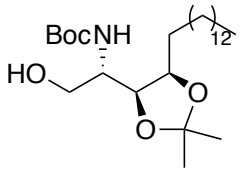
Triol **51** (5.32 g, 12.8 mmol) was dissolved in pyridine (50 mL). TBDPSCl (4.00 mL, 15.8 mmol) was added to the solution followed by DMAP (2 crystals). The reaction mixture was stirred at 20 °C for 16 h. The reaction was quenched by the addition of H_2O (50 mL) before being separated using EtOAc (50 mL). The aqueous layer was extracted with EtOAc (50 mL × 2). The combined organic layers were dried over Na_2SO_4, filtered and concentrated under reduced pressure. The resulting crude mixture was purified by flash column chromatography (0->20% hexane:EtOAc) to afford silyl ether **52** as a colourless oil (6.19 g, 73%): *Rf* = 0.4 (hexane:EtOAc 4:1); δ_H ($CDCl_3$, 300 MHz) 0.87 (t, *J* = 6.6 Hz, 3H), 1.06 (s, 9H), 1.25 (br s, 23H), 1.41 (s, 9H), 1.46-1.56 (m, 2H), 1.62-1.74 (m, 1H), 2.62 (br s, OH), 3.11 (br s, OH), 3.58-3.68 (m, 2H), 3.76-3.89 (m, 2H), 3.92-4.02 (m, 1H), 5.17 (d, J = 8.4 Hz, NH), 7.34-7.46 (m, 6H), 7.60-7.68 (m, 4H); δ_C NMR ($CDCl_3$, 100 MHz) δ 14.1, 19.1, 22.7, 25.9, 26.8, [28.3, 29.3, 29.5, 29.6, 29.7, 31.9, 33.1, resonance overlap], 52.0, 64.0, 73.4, 75.6, 79.6, 127.9, 129.97, 127.98, 132.3, 132.5, 135.5, 135.53, 155.7; LR-MS (TOF ES+) *m/z* calcd for $C_{39}H_{65}NNaO_5Si$ $[M + Na]^+$ 678.4, found 678.4 ($[M + Na]^+$, 100%)

***tert*-butyl ((*S*)-2-((*tert*-butyldiphenylsilyl)oxy)-1-((4*S*,5*R*)-2,2-dimethyl-5-tetradecyl-1,3-dioxolan-4-yl)ethyl)carbamate (53)**



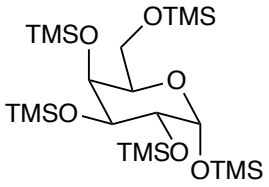
Diol **52** (6.19 g, 9.3 mmol) was dissolved in 2,2 dimethoxypropane (50 mL). Camphorsulfonic acid (310 mg, 1.34 mmol) was added to the solution and the pH was checked using litmus paper to ensure the pH was not lower than 3. The resulting solution was stirred at 20 °C for 4 h and then quenched by the addition of Et_3N before being concentrated under reduced pressure. The resulting clear yellow oil was purified by flash column chromatography (0->20% hexane:EtOAc) to afford acetal **53** as a colourless oil (4.59 g, 71%). *Rf* = 0.8 (hexane:EtOAc 5:1); δ_H ($CDCl_3$, 300 MHz) 0.87 (t, *J* = 6.5 Hz, 3H), 1.05 (s, 9H), 1.25 (br s, 27H), 1.35 (s, 3H), 1.42 (s, 3H), 1.45 (s, 9H), 3.72 (d, *J* = 9.9 Hz, 1H), 3.80 (d, *J* = 9.9 Hz, 1H), 3.89 (dd, *J* = 9.9, 3.3 Hz, 1H), 4.18 (dd, *J* = 9.9, 3.3 Hz, 1H), 4.78 (d, *J* = 10.0 Hz, 1H), 7.27 - 7.51 (m, 6H), 7.66 (m, 4H); δ_C ($CDCl_3$, 100 MHz) 14.1, 22.7, 25.3, 26.7, 27.6, 28.4, 29.2, 29.3, 29.5, 29.6, 29.6, 29.7, 31.9, 51.1, 63.9, 77.9, 78.3, 81.2, 127.9, 129.9, 127.9, 132.3, 132.5, 135.5, 135.5, 156.4 LR-MS (TOF ES+) *m/z* calcd for $C_{42}H_{69}NNaO_5Si$ $[M + Na]^+$ 718.4, found 718.4 ($[M + Na]^+$, 100%)

***tert*-butyl ((*S*)-1-((4*S*,5*R*)-2,2-dimethyl-5-tetradecyl-1,3-dioxolan-4-yl)-2-hydroxyethyl)carbamate (47)**



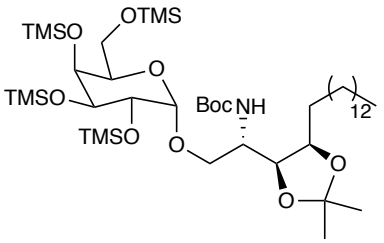
Silyl ether **53** (4.59 g, 6.6 mmol) was dissolved in THF (50 mL). Upon the addition of TBAF (1 M in THF, 20 mL, 20.0 mmol) the clear solution turned clear yellow. The resulting solution was stirred for 16 h. The reaction was then quenched by the addition of brine (50 mL), the THF was then removed under reduced pressure. EtOAc (50 mL) was added and the mixture was separated. The resulting aqueous layer was extracted with EtOAc (2 × 50 mL). The combined organic layers were dried over Na_2SO_4, filtered and concentrated under reduced pressure. The crude mixture was purified via flash column chromatography (0->20% hexane:EtOAc), to afford alcohol **47** as a white solid (2.03 g, 67%). *Rf* = 0.3 (hexane:EtOAc 3:2); δ_H ($CDCl_3$, 300 MHz) 0.88 (t, *J* = 6.9 Hz, 3H), 1.32 (s, 3H), 1.46 (s, 3H), 1.47 (s, 9H), 1.70-1.21 (m, 26H), 2.23 (br s, 1H), 3.70 (m, 1H), 3.38 (m, 1H), 3.77 (m, 1 H) 3.86 (m, 1H), 4.19 (m, 1 H), 4.93 (d, *J* = 8.5 Hz, 1H); δ_C ($CDCl_3$, 100 MHz) 14.1, 22.7, 25.3, 26.7, [27.6, 28.4, 29.2, 29.3, 29.5, 29.6, 29.6, 29.7, resonance overlap], 31.9, 51.1, 63.9, 77.9, 78.3, 81.2, 108.7, 156.4; LR-MS (TOF ES+) *m/z* calcd for $C_{26}H_{51}NNaO_5$ $[M + Na]^+$ 480.4, found 480.4 ($[M + Na]^+$, 100%)

(((2*R*,3*R*,4*S*,5*S*,6*R*)-6-(((trimethylsilyl)oxy)methyl)tetrahydro-2*H*-pyran-2,3,4,5-tetrayl)tetrakis(oxy))tetrakis(trimethylsilane) (49)



D-Galactose (4.40 g, 24.4 mmol) was dissolved in HMDS and anhydrous pyridine (100 mL 1:1). TMSCl (25 mL, 250 mmol) was added and the reaction mixture was heated to 65 °C and stirred for 16 h. The reaction mixture was then quenched by pouring into ice-cold water (400 mL) before being extracted with hexane (3 × 300 mL). The combined organic layers were then dried over Na_2SO_4, filtered and concentrated under reduced pressure. The resulting clear oil was used without further purification (11.5 g, 87%).

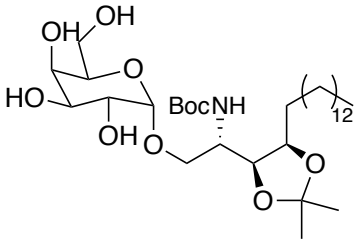
***tert*-butyl ((*S*)-1-((4*S*,5*R*)-2,2-dimethyl-5-tetradecyl-1,3-dioxolan-4-yl)-2-(((2*S*,3*R*,4*S*,5*S*,6*R*)-3,4,5-tris((trimethylsilyl)oxy)-6-(((trimethylsilyl)oxy)methyl)tetrahydro-2*H*-pyran-2-yl)oxy)ethyl)carbamate 46**



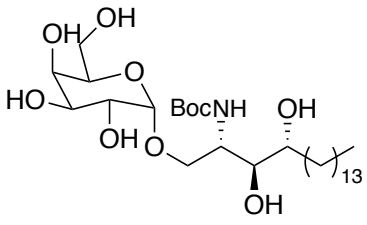
TMSI (2.25 mL, 15.7 mmol) was added to a solution of per-silylated galactose **49** (7.10 g, 10.5 mmol) in CH_2Cl_2 (40 mL) at 0 °C. The reaction mixture was stirred under an Ar atmosphere for 15 min before benzene (40 mL) was added. The solvent was removed under reduced pressure and the resulting

glycosyl iodide intermediate **48** was dissolved in CH_2Cl_2 (40 mL) and kept under an Ar atmosphere. In a separate flask, a mixture of activated 4 Å molecular sieves (7.20 g), *n*-Bu_4NI (7.27 g, 19.7 mmol), *i*-Pr_2NEt (3.40 mL, 19.7 mmol) and alcohol **47** (1.73 g, 3.8 mmol) in CH_2Cl_2 (40 mL) was prepared and stirred under an Ar atmosphere at 25 °C for 15 min. The solution of glycosyl iodide **48** in CH_2Cl_2 was then added dropwise over 5 min to this mixture and the resulting mixture was stirred overnight. After removal of the solvent under reduced pressure, Et_2O (50 mL) and H_2O (50 mL) were added and the phases were separated. The organic phase was dried over Na_2SO_4, filtered and then concentrated under reduced pressure. Purification by flash column chromatography proved difficult and was not possible. (1.76 g, 61%). *Rf* = 0.8 (hexane:EtOAc 5:1); LR-MS (TOF ES+) *m*/*z* calcd for $C_{44}H_{94}NO_{10}Si_4$ $[M + H]^+$ 908.6, found 908.6 ($[M + H]^+$, 10%) calcd for $C_{44}H_{93}NNaO_{10}Si_4$ $[M + Na]^+$ 930.6, found 930.6 ($[M + Na]^+$, 100%)

***tert*-butyl ((*S*)-1-((4*S*,5*R*)-2,2-dimethyl-5-tetradecyl-1,3-dioxolan-4-yl)-2-(((2*S*,3*R*,4*S*,5*R*,6*R*)-3,4,5-trihydroxy-6-(hydroxymethyl)tetrahydro-2*H*-pyran-2-yl)oxy)ethyl)carbamate (55) and *tert*-butyl ((2*S*,3*S*,4*R*)-3,4-dihydroxy-1-(((2*S*,3*R*,4*S*,5*R*,6*R*)-3,4,5-trihydroxy-6-(hydroxymethyl)tetrahydro-2*H*-pyran-2-yl)oxy)octadecan-2-yl)carbamate (56)**



55



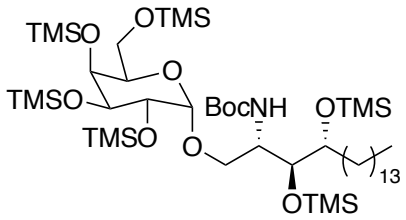
56

Glycoside **46** (1.76 g, 2.32 mmol) was dissolved in a solution of $CHCl_3$:MeOH:HCl (aq) (80 mL, 10:10:3) and the resulting solution was stirred for 4 h. The reaction was partitioned by the addition of $CHCl_3$ (35 mL) and H_2O (15 mL). The organic phase was isolated, concentrated under reduced pressure and the crude material was purified by flash column chromatography (0->15% CH_3Cl:MeOH 9:1) to yield, in order of elution, acetal **21** as a colourless oil (215 mg, 15%). Acetal **55)** *Rf* = 0.3 (CH_3Cl:MeOH 9:1); δ_H ($CDCl_3$:CD_3OD, 2:1, 300 MHz) 1.06-1.16 (stack, 22H), 1.24-1.32 (m, 19H), 3.26 (m 1H), 3.51-3.64 (stack, 3H), 3.65-3.98 (stack, 7H), 4.89 (d, *J* = 3.3 Hz, 1H), exchangeable protons not observed; LR-MS (TOF ES+) *m*/*z* calcd for $C_{32}H_{61}NNaO_{10}$ $[M + Na]^+$ 642.4, found 642.4 ($[M + Na]^+$,100%) No ^{13}C spectrum recorded

Pentaol 56) (711 mg, 53%) *Rf* = 0.2 (CH_3Cl:MeOH 9:1); δ_H ($CDCl_3$:CD_3OD, 2:1, 300 MHz) 0.85 (t, *J* 6.9, 3H), 1.06-1.16 (stack, 22H), 1.24 (s, 9H), 1.25-1.38 (stack, 4H), 3.26 (m, 1H), 3.51-3.64 (stack, 3H), 3.65-3.98 (stack,

7H), 4.89 (d, *J* = 3.3 Hz, 1H), exchangeable protons not observed; LR-MS (TOF ES+) *m/z* calcd for $C_{29}H_{57}NNaO_{10}$ $[M + Na]^+$ 602.4, found 602.4 ($[M + Na]^+$ 100%) No ^{13}C spectrum recorded

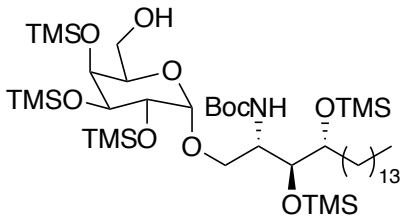
tert-butyl ((2*S*,3*S*,4*R*)-3,4-bis((trimethylsilyl)oxy)-1-(((2*S*,3*R*,4*S*,5*S*,6*R*)-3,4,5-tris((trimethylsilyl)oxy)-6-(((trimethylsilyl)oxy)methyl)tetrahydro-2*H*-pyran-2-yl)oxy)octadecan-2-yl)carbamate (57)



Pentaol 56 (711 mg, 1.2 mmol) was dissolved in HDMS:pyridine (100 mL, 1:1) and the resulting solution was stirred at 25 °C. TMSCl (2.11 mL, 16.6 mmol) was added dropwise, over 5 min, to the solution, which was then stirred for 18 h. The mixture was then poured into ice-water (500 mL) and extracted with hexane (3 × 300 mL). The combined organic extracts were washed with brine (300 mL), dried over Na_2SO_4, filtered and concentrated under reduced pressure to afford per-silylated galactoside **57** as a colourless oil (776 mg, 73%). *Rf* = 0.4 (hexane:EtOAc 95:5); δ_H ($CDCl_3$, 300 MHz) 0.10 (s, 9H), 0.11 (s, 9H), 0.12 (s, 9H), 0.13 (s, 9H), 0.14 (s, 9H), 0.15 (s, 9H), 0.85 (t, *J* = 6.9 Hz, 3H), 1.26-1.26 (stack, 22H), 1.41-1.43 (stack, 4H), 3.53-3.60 (m, 1H), 3.62-3.83 (m, 7H), 3.84-3.98 (m, 3H), 4.67 (d, *J* = 3.3 Hz, 1H) 5.14 (d, *J* = 5.1 Hz, 1H); δ_C ($CDCl_3$, 100 MHz) -0.3 -0.2, 0.0 (overlap), 0.2, 13.6, 22.2, 25.7, 27.9, 28.8, 29.2, 31.5, 51.9, 62.6, 68.9, 70.0, 70.4, 71.5, 72.9,

73.9, 76.1, 102.1, 155.4; LR-MS (TOF ES+) *m/z* calcd for $C_{47}H_{106}NO_{19}Si_6$ [M + H]$^+$ 1012.7, found 1012.7 ([M + H]$^+$, 10%), calcd for $C_{47}H_{105}NO_{19}Si_6Na$ [M + Na]$^+$ 1034.6, found 1034.6 ([M + Na]$^+$, 100%); HRMS (TOF ES+) calcd for $C_{47}H_{105}NO_{19}Si_6Na$ [M + Na]$^+$ 1034.6248, found 1034.6252

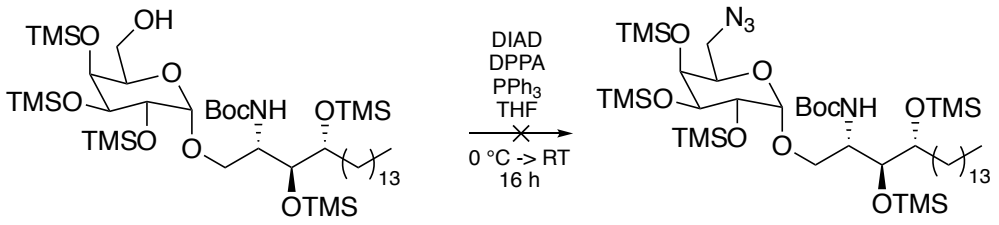
***tert*-butyl ((2*S*,3*S*,4*R*)-1-(((2*S*,3*R*,4*S*,5*S*,6*R*)-6-(hydroxymethyl)-3,4,5-tris((trimethylsilyl)oxy)tetrahydro-2*H*-pyran-2-yl)oxy)-3,4-bis((trimethylsilyl)oxy)octadecan-2-yl)carbamate (58)**



Per-silylated galactoside 57 (776 mg, 0.83 mmol) was dissolved in CH_2Cl_2 and MeOH (40 mL, 1:3) and the resulting solution was cooled to 0 °C. K_2CO_3 (30 mg) was added and the reaction mixture was stirred for 30 min. The reaction was then quenched by the addition of glacial acetic acid (1 mL) before being rapidly concentrated under reduced pressure. The crude product was purified by flash column chromatography (0->5% hexane:EtOAc) to yield alcohol **58** as a colourless oil (441 mg, 62%). *Rf* = 0.5 (hexane:EtOAc 9:1); δ_H ($CDCl_3$, 300 MHz) 0.09 (s, 9H), 0.11 (s, 9H), 0.12 (s, 9H), 0.13 - 0.15 (stack, 18H) 0.87 (t, *J* = 6.9 Hz, 3H), 1.23-1.26 (stack, 22H), 1.41-1.43 (stack, 4H), 3.56-3.64 (m, 1H), 3.68-3.84 (m, 7H), 3.86-3.93 (m, 3H), 4.74 (d, *J* = 3.3 Hz, 1H), 5.17 (d, *J* = 5.1 Hz, 1H); δ_C ($CDCl_3$, 100 MHz) -0.2, 0.0 (overlap), 0.2, 13.6, 22.2, 25.7, [27.9, 28.8, 29.2, resonance overlap], 31.5, 51.9, 62.6, 68.9, 70.0, 70.4, 71.5, 72.9, 73.9, 76.1, 102.1, 155.4; LR-MS (TOF ES+) *m/z* calcd

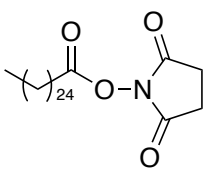
for $C_{41}H_{90}NO_{10}Si_4$ $[M + H]^+$ 940.6, found 940.6 ($[M + H]^+$, 10%) calcd for $C_{41}H_{89}NO_{10}Si_4Na$ $[M + Na]^+$ 962.6, found 962.6 ($[M + Na]^+$, 100%); HRMS (TOF ES+) calcd for $C_{41}H_{89}NO_{10}Si_4Na$ $[M + Na]^+$ 962.5852, found 962.5857 $C_{41}H_{89}NO_{10}Si_4$

Attempted Mitsunobu reaction to *tert*-butyl ((2*S*,3*S*,4*R*)-1-(((2*S*,3*R*,4*S*,5*S*,6*R*)-6-(azidomethyl)-3,4,5-tris((trimethylsilyl)oxy)tetrahydro-2*H*-pyran-2-yl)oxy)-3,4-bis((trimethylsilyl)oxy)octadecan-2-yl)carbamate (59)



PPh_3 (490 mg, 1.86 mmol), followed by DIAD (365 µL, 1.86 mmol) and then DPPA (400 µL, 1.86 mmol) were added sequentially to a solution of alcohol **58** (441 mg, 0.55 mmol) in THF (20 mL) at 0 °C. The mixture was allowed to warm to RT and stirred for 18 h. The reaction mixture was then concentrated under reduced pressure.

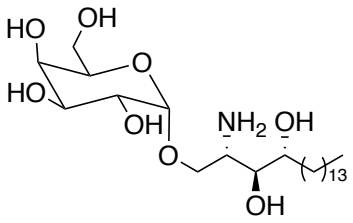
2,5-dioxopyrrolidin-1-yl hexacosanoate (61)



Hexacosanoic acid (500 mg, 1.26 mmol) was dissolved in CH_2Cl_2 (30 mL), 1-Ethyl-3-(3-dimethylaminopropyl)carbodiimide hydrochloride (270 mg, 1.35

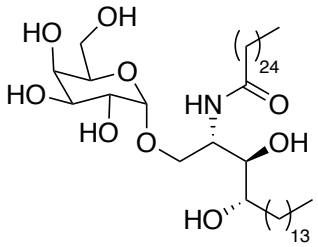
mmol) and *N*-hydroxysuccinimide (175 mg, 1.50 mmol) were added sequentially. The reaction mixture was heated at 40 °C for 18 h and then the mixture was poured into water (20 mL) and extracted with Et_2O (60 mL). The organic layer was washed with brine (20 mL), dried over Na_2SO_4, and filtered. The solvent was removed under reduced pressure to give a white foam (0.59 g, 95%).

(2*S*,3*R*,4*S*,5*R*,6*R*)-2-(((2*S*,3*S*,4*R*)-2-amino-3,4-dihydroxyoctadecyl)oxy)-6-(hydroxymethyl)tetrahydro-2*H*-pyran-3,4,5-triol (62)



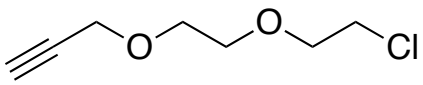
TFA (1.0 mL, 13.2 mmol) was added dropwise over 5 min to galactoside **55** (215 mg, 0.34 mmol) at 25 °C. After 30 min, the reaction mixture was concentrated under reduced pressure. The resulting colourless oil was used in the next step without further purification (166 mg, 100%).

***N*-((2*S*,3*S*,4*R*)-3,4-dihydroxy-1-(((2*S*,3*R*,4*S*,5*R*,6*R*)-3,4,5-trihydroxy-6-(hydroxymethyl)tetrahydro-2*H*-pyran-2-yl)oxy)octadecan-2-yl)hexacosanamide (KRN7000 (36))**



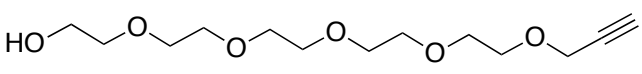
Amine **62** (166 mg, 0.34 mmol) and Et_3N (0.72 mL, 5.1 mmol) were added to a stirred solution of NHS ester **61** (170 mg, 1.7 mmol) in THF (25 mL). The reaction mixture was stirred at 50 °C for 18 h. The reaction mixture was then concentrated under reduced pressure. The crude material purified by flash column chromatography ($CHCl_3$:MeOH 0->15%) to yield **KRN7000** (187 mg, 63%); R_f 0.60 (MeOH/$CHCl_3$ = 1:4); δ_H (400 MHz, $CDCl_3$:CD_3OD, 2:1) 0.86 (t, *J* = 6.6 Hz, 6H), 1.24 (stack, 66H), 1.51-1.64 (m, 5H), 2.19 (t, *J* = 7.7 Hz, 2H), 3.47 - 3.62 (m, 3H), 3.65 - 3.79 (m, 7H), 3.84 - 3.93 (m, 2H), 4.14 - 4.21 (m, 1H), 4.88 (d, *J* = 3.6 Hz, 2H); δ_C ($CDCl_3$:CD_3OD, 2:1, 100 MHz) 13.7, 22.5, 25.7, 25.8, 29.2, 29.3, 29.4, 29.5 (resonance overlap, alkyl chain), 31.8, 32.3, 36.3, 50.4, 61.4, 67.2, 68.8, 69.7, 70.1, 70.7, 71.8, 74.5, 99.7, 174.5; (TOF ES+) *m*/*z* calcd for $C_{50}H_{98}NNaO_9$ $[M + Na]^+$ 879.7, found 879.7 ($[M + Na]^+$, 100%)

3-(2-(2-chloroethoxy)ethoxy)prop-1-yne (68a)



2-(2-Chloroethoxy)ethanol (1.00 g, 8.1 mmol) was dissolved in THF (30 mL) and the mixture was cooled to 0 °C. Upon addition of sodium hydride (0.193 g, 8.1 mmol, 60% dispersion in mineral oil) the solution turned a brick red colour. The reaction mixture was stirred for 30 min before the dropwise addition of propargyl bromide over 5 min (0.72 mL, 8.1 mmol). The solution was stirred for 2 h at 0 °C before being warmed to 25 °C and stirred for a further 20 h. The mixture was poured into water (50 mL), extracted with CH_2Cl_2 (40 mL) and dried over Na_2SO_4, filtered and concentrated under reduced pressure. The crude material was purified via flash column chromatography (0->25 hexane:EtOAc) to afford alkyne **68a** as a colourless oil. *Rf* = 0.4 (hexane:EtOAc 3:1); δ_H ($CDCl_3$, 300 MHz); 2.37 (t, *J* = 2.3 Hz, 1H), 3.54 - 3.73 (8H, m), 4.15 (d, *J* = 2.3 Hz, 2H); δ_C ($CDCl_3$, 100 MHz) 42.6, 58.2, 68.8, 70.2, 71.1, 74.6, 79.4; LR-MS (TOF ES+) *m/z* calcd for $C_7H_{12}ClO_2$ $[M + H]^+$ 163.1, found 163.1 ($[M + H]^+$, 100%)

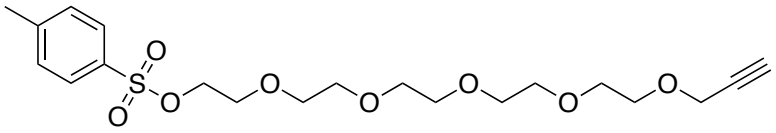
3,6,9,12,15-pentaoxaoctadec-17-yn-1-ol (71)



Pentaethylene glycol (1.00 g, 4.1 mM) was dissolved in THF (30 mL) and the mixture was cooled to 0 °C. Upon addition of sodium hydride (79 mg, 3.3 mmol) the solution turned a brick red colour. The reaction mixture was allowed to stir for 30 min before the dropwise addition of propargyl bromide over 5 min

(0.29 mL, 3.3 mmol). The solution was stirred for 2 h at 0 °C before being warmed to 25 °C and stirred for a further 20 h. The mixture was poured into water (50 mL), extracted with CH_2Cl_2 (40 mL) and dried over Na_2SO_4, filtered and concentrated under reduced pressure. The resulting crude material was purified by flash column chromatography (0->25% hexane:EtOAc) to yield **71** as a clear yellow liquid (0.88 g, 76%); R_f = 0.3 (hexane:EtOAc 3:1); δ_H ($CDCl_3$, 300 MHz) 2.31 (t, *J* = 2.3 Hz, 1H), 3.56 - 3.58 (m, 12H) 3.59 - 3.63 (m, 6H), 4.10 - 4.15 (m, 4H); δ_C ($CDCl_3$, 100 MHz) 58.3, 61.5, 63.5, 69.1, 70.1, 70.3, 70.5 [resonance overlap], 72.7, 74.6, 79.5; LR-MS (TOF ES+) *m*/*z* calcd for $C_{13}H_{25}O_6$ $[M + H]^+$ 277.2, found 277.2 ($[M + H]^+$ 100%)

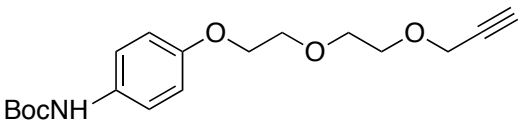
3,6,9,12,15-pentaoxaoctadec-17-yn-1-yl 4-methylbenzenesulfonate (68b)



Alcohol **71** (0.88 g, 3.2 mmol) was dissolved in CH_2Cl_2 (20 mL), Et_3N (1.20 mL, 8.5 mmol) and tosyl chloride (980 mg, 5.6 mmol) were added and the mixture was stirred under Ar for 15 h. The mixture was washed sequentially with satd $NaHCO_3$ solution (50mL) and water (50 mL). Organic layer was dried over Na_2SO_4, filtered and the solvent removed under reduced pressure. The resulting crude material was purified by flash column chromatography (0->20% hexane:EtOAc) to yield **tosylate 68b** as a clear yellow oil (1.11 g, 81%) *Rf* = 0.8 (hexane:EtOAc 3:1); δ_H ($CDCl_3$, 300 MHz) 2.36 (t, *J* = 2.5 Hz, 1H) 2.38 (s, 3H), 3.50 - 3.63 (m, 18H), 4.07 - 4.10 (m, 2H), 4.13 (d, *J* = 2.5 Hz, 2H) 7.25 - 7.29 (m, 2H, AA' of AA'BB') 7.71 - 7.75 (m, 2H, BB' of AA'BB'); δ_C ($CDCl_3$, 100 MHz) 21.6, 58.4, 68.7, 69.1, 69.2, [70.4, 70.5, 70.61, 70.64, 70.8,

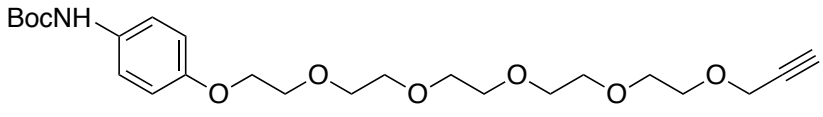
resonance overlap], 74.5, 79.7, 128.0, 129.8, 133.0, 144.8; LR-MS (TOF ES+) *m/z* calcd for $C_{20}H_{30}NaO_8S$ $[M + Na]^+$ 453.2, found 453.2 ($[M + Na]^+$, 100%)

tert-butyl (4-(2-(2-(prop-2-yn-1-yloxy)ethoxy)ethoxy)phenyl)carbamate (66a)



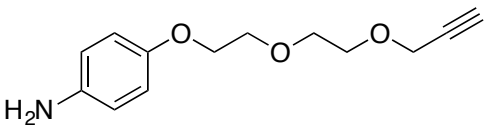
To a solution of *N*-Boc-4-aminophenol (1.68 g, 8.0 mmol) in DMF (50) was added alkyne **68a** (1.04 g, 6.45 mmol) and K_2CO_3 (3.32 g, 24.02 mmol). The mixture was stirred at 60 °C for 18 h, after which 1M HCl (aq) (30 mL) was added. The mixture was then extracted with EtOAc (2 × 40 mL), dried over anhydrous Na_2SO_4, filtered, and then concentrated under reduced pressure. The resulting crude material was purified by flash column chromatography (0->40% hexane:EtOAc) to yield carbamate **66a** as a colourless oil (1.45 g, 53%) *Rf* = 0.5 (hexane:EtOAc 3:2); δ_H ($CDCl_3$, 300 MHz) 1.46 (s, 9H), 2.42 (t, *J* = 2.3 Hz, 1H), 3.51-3.71 (m, 4H) 3.74-79 (m, 2H), 4.00 4.06 (m, 2H), 4.13 (d, *J* = 2.3 Hz, 2H), 6.36 (br. s, 1H), 6.73 - 6.81 (m, 2H, AA' of AA'BB'), 7.06-7.28 (m, 2H, BB' of AA'BB') No ^{13}C spectrum recorded; (TOF ES+) *m/z* calcd for $C_{18}H_{25}NNaO_5$ $[M + Na]^+$ 358.2, found 358.2 ($[M + Na]^+$, 100%)

tert-butyl (4-((3,6,9,12,15-pentaoxaoctadec-17-yn-1-yl)oxy)phenyl)carbamate (66b)



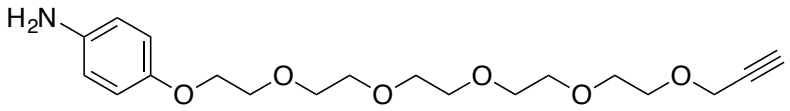
N-Boc-4-aminophenol (0.54 g, 2.6 mmol) was added to a solution of **68b** (1.12 g, 2.58 mmol) and K_2CO_3 (1.07 g, 7.74 mmol) in DMF (50 mL). The mixture was stirred at 60 °C for 18 h, after which 1M HCl (aq) (30 mL) was added. The mixture was then extracted with EtOAc (2 × 40 mL), dried over anhydrous Na_2SO_4, filtered, and then concentrated under reduced pressure. The resulting crude material was purified by flash column chromatography (0->20% hexane:EtOAc) to yield carbamate **66b** as a clear yellow oil (0.59 g, 49%) *Rf* = 0.8 (hexane:EtOAc 3:1) δ_H ($CDCl_3$, 300 MHz) 1.46 (s, 9H), 2.36 (t, *J* = 2.5 Hz, 1H) 2.38 (s, 3H), 3.50 - 3.63 (m, 18H), 4.07 - 4.10 (m, 2H), 4.13 (d, *J* = 2.5 Hz, 2H) 7.25 - 7.29 (m, 2H, AA' of AA'BB') 7.71 - 7.75 (m, 2H, BB' of AA'BB'). No ^{13}C spectrum recorded; (TOF ES+) *m/z* calcd for $C_{24}H_{37}NNaO_8$ [M + Na]$^+$ 490.2, found 490.2 ([M + Na]$^+$, 100%)

4-(2-(2-(prop-2-yn-1-yloxy)ethoxy)ethoxy)aniline (65a)



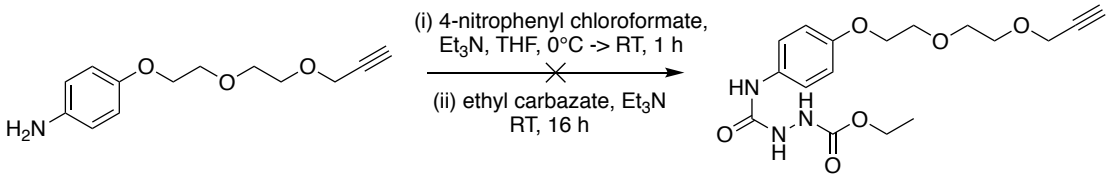
TFA (5 mL) was added, dropwise over 5 min, a solution of **66a** (1.14 g, 3.42 mmol) in CH_2Cl_2 (20 mL). The mixture was stirred at 25 °C for 2 h before being concentrated under reduced pressure to afford amine **65a** with a quantitative yield. The crude material was used without further purification.

4-((3,6,9,12,15-pentaoxaoctadec-17-yn-1-yl)oxy)aniline (65b)



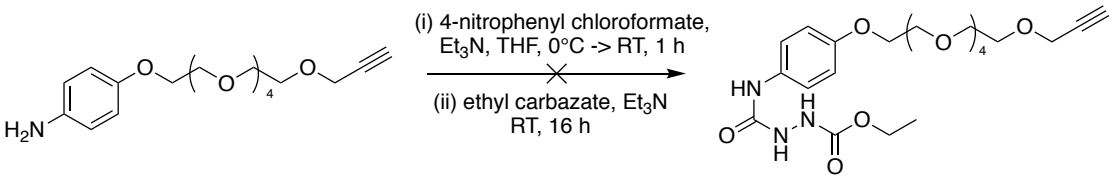
TFA (5 mL) was added, dropwise over 5 minutes, a solution of **66a** (0.59 g, 1.27 mmol) in CH_2Cl_2 (20 mL). The mixture was stirred at 25 °C for 2 h before being concentrated under reduced pressure to afford amine **65b** with a quantitive yield. The crude material was used without further purification

ethyl 2-((4-(2-(2-(prop-2-yn-1-yloxy)ethoxy)ethoxy)phenyl)carbamoyl)hydrazine-1-carboxylate (64a)



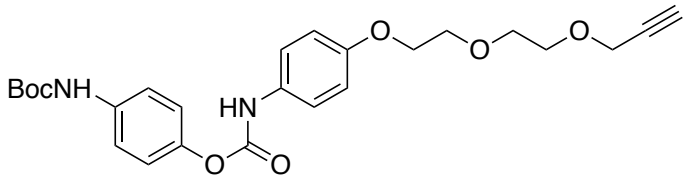
4-nitrophenyl chloroformate (2.06 g, 10.24 mmol) and Et_3N (1.42 mL, 10.3 mmol were added sequentially to a solution of amine **65a** (0.80 g, 3.4 mmol) in THF (40 mL) at 0 °C. The mixture was stirred at 25 °C for 1 h. Then ethyl carbazate (1.54 g, 14.8 mmol) and Et_3N (1.42 mL, 10.3 mmol) were added. The mixture was stirred at 25 °C for 16 h. The reaction mixture was concentrated under reduced pressure then diluted with satd. $NaHCO_3$ solution and extracted with EtOAc (2 × 30 mL) before being dried over anhydrous Na_2SO_4, filtered, and concentrated under reduced pressure.

ethyl 2-((4-((3,6,9,12,15-pentaoxaoctadec-17-yn-1-yl)oxy)phenyl)carbamoyl)hydrazine-1-carboxylate (64b)



4-nitrophenyl chloroformate (0.76 g, 3.8 mmol) and Et_3N (0.52 mL, 3.8 mmol) were added to a solution of **65b** (0.46 g, 1.7 mmol) in THF (40 mL) at 0 °C. The mixture was stirred at 25°C for 1 h. Then ethyl carbazate (0.57 g, 5.4 mmol) and Et_3N 0.52 mL, 3.8 mmol) were added. The mixture was stirred at 25 °C for 16 h. The reaction mixture was concentrated under reduced pressure then diluted with satd. $NaHCO_3$ solution and extracted with EtOAc (2 × 30 mL) before being dried over anhydrous Na_2SO_4, filtered, and concentrated under reduced pressure.

4-((*tert*-butoxycarbonyl)amino)phenyl (4-(2-(2-(prop-2-yn-1-yloxy)ethoxy)ethoxy)phenyl)carbamate (73)



4-nitrophenyl chloroformate (1.28 g, 6.36 mmol) and Et_3N (0.88 mL, 6.36 mmol) were added sequentially to a solution of 65**a** (0.50 g, 2.1 mmol) in THF (40 mL) at 0 °C. The mixture was stirred at 25°C for 18 h. The reaction mixture was concentrated under reduced pressure then diluted with satd. $NaHCO_3$ solution and extracted with EtOAc (2 × 30 mL) before being dried over anhydrous Na_2SO_4, filtered, and concentrated under reduced pressure. The crude material was purified by flash column chromatography

(hexane:EtOAc, 0->25%) to afford carbamate as a red oil. *Rf* = 0.3 (hexane:EtOAc 3:1); δ_H (300 MHz, $CDCl_3$) 1.50 (s, 9H) 2.42 (t, 1H, *J* = 2.5 Hz) 3.70 - 3.77 (m, 4H) 3.84 (t, *J* = 4.9 Hz, 2H) 4.10 (t, J = 4.9 Hz, 2H) 4.20 (d, *J* = 2.5 Hz, 2H) 6.53 (br s, 1H) 6.84 - 6.93 (m, 2H) 7.06 - 7.11 (m, 2H) 7.29 - 7.39 (m, 4H); δ_C ($CDCl_3$, 100 MHz) 28.3, 58.5, 67.8, 69.1, 69.8, 70.6, 74.6, 79.7, 80.6, 115.2, 119.2, 120.5, 122.1, 130.7, 135.8, 146.0, 152.8, 155.5; LR-MS (TOF ES+) *m/z* calcd for $C_{25}H_{30}N_2NaO_7$ $[M + Na]^+$ 493.6, found 493.6 ($[M + Na]^+$, 100%)